

Doctoral Thesis at the Medical University of Vienna for obtaining the Degree

‘Doctor of Philosophy - PhD’

# **Complement Factor H binds malondialdehyde- epitopes and protects from oxidative stress**

Author

**David Weismann, Mag. rer. nat.**

Supervisor

**Univ. Prof. Christoph J. Binder, MD, PhD**

**Ce-M-M-**

Research Center for Molecular Medicine  
of the Austrian Academy of Sciences

**KILM**

Department of Laboratory Medicine  
Medical University of Vienna

Lazarettgasse 14, AKH BT 25.3

1090 Vienna, Austria

Vienna, July 2011



# TABLE OF CONTENTS

<b>1. ABSTRACT .....</b>	<b>5</b>
1.1 Abstract – English.....	5
1.2 Kurzfassung –Deutsch .....	5
<b>2. INTRODUCTION .....</b>	<b>7</b>
2.1 Sterile inflammation and danger-associated molecular patterns.....	7
2.2 Oxidation-specific epitopes are targets of innate immunity.....	8
2.3 Generation of Malondialdehyde-adducts .....	10
2.4 Age-related macular degeneration .....	11
2.5 Complement system.....	13
2.6 Complement Factor H.....	14
<b>3. AIM OF THE STUDY.....</b>	<b>17</b>
<b>4. METHODS.....</b>	<b>18</b>
4.1 Subjects and Clinical Diagnosis.....	18
4.2 Plasma Samples .....	19
4.3 Genotyping.....	20
4.4 Intravitreal injection.....	20
4.5 Proteins and antibodies .....	21
4.6 Bead coupling and pulldown-procedure .....	22
4.7 Immunoblotting.....	23
4.8 Immunoassay .....	23
4.9 Competition immunoassay.....	24
4.10 Immunohistochemistry and confocal microscopy .....	25
4.11 Microparticle isolation and staining.....	26
4.12 Co-factor assay.....	26
4.13 Macrophage foam cell assay .....	26

4.14 Macrophage binding assay.....	27
4.15 Cell stimulations .....	28
4.16 Statistical analysis.....	29
<b>5. RESULTS .....</b>	<b>30</b>
5.1 CFH binds to MDA in mouse and human plasma .....	30
5.2 CFH interacts directly with MDA-modifications .....	30
5.3 CFH interacts specifically with MDA-modifications .....	33
5.4 CFH interacts with MDA via SCR 7 and SCR20 .....	35
5.5 The AMD-associated CFH SNP rs1061170 leads to impaired binding to MDA .....	37
5.6 CFH binds cellular debris via MDA-epitopes.....	39
5.7 CFH inactivates complement on MDA-bearing surfaces .....	42
5.8 CFH inhibits MDA-induced responses in vitro .....	44
5.9 CFH inhibits MDA-induced responses in vivo.....	47
<b>6. DISCUSSION .....</b>	<b>49</b>
<b>7. FUTURE DIRECTIONS.....</b>	<b>54</b>
<b>8. REFERENCES .....</b>	<b>56</b>
<b>9. LIST OF ABBREVIATIONS.....</b>	<b>62</b>
<b>10. PUBLICATION BASED ON THE THESIS .....</b>	<b>63</b>
<b>11. ACKNOWLEDGEMENTS .....</b>	<b>64</b>
<b>12. FUNDING.....</b>	<b>65</b>
<b>13. AUTHORS CURRICULUM VITAE.....</b>	<b>66</b>

# 1. ABSTRACT

## 1.1 Abstract – English

Oxidative stress and enhanced lipid peroxidation are linked to many chronic inflammatory diseases, including age-related macular degeneration (AMD). AMD is the leading cause of blindness in western societies, but its etiology remains largely unknown. Malondialdehyde (MDA) is a common lipid peroxidation product that accumulates in many pathophysiological processes including AMD. I identified complement factor H (CFH) as a major MDA-binding protein that can block both the uptake of MDA-modified proteins by macrophages *in vitro* as well as MDA-induced proinflammatory effects *in vivo*. The CFH polymorphism H402, which is strongly associated with AMD, dramatically reduces the ability of CFH to bind MDA, thereby suggesting a causal link to disease etiology. The findings included in this thesis provide important mechanistic insights into innate immune responses to oxidative stress, which may be exploited in the prevention and therapy of AMD and other chronic inflammatory diseases.

## 1.2 Kurzfassung –Deutsch

Oxidativer Stress und die damit verbundene Lipidperoxidation treten in vielen chronisch-entzündlichen Erkrankungen auf. Ein Beispiel dafür ist die altersbedingte Makuladegeneration (AMD). AMD ist die Hauptursache für Erblindung in Industriestaaten. Trotz intensiver Forschung bleibt ihre Pathogenese ungeklärt. Malondialdehyd (MDA) ist ein Lipidperoxidationsprodukt, das in entzündlichen Prozessen, wie der AMD, vermehrt gebildet wird. In dieser Dissertation wird die Identifikation von Komplementfaktor H (CFH) als MDA-bindendes Plasmaprotein berichtet, welches sowohl die Aufnahme von MDA-modifizierten Proteinen durch Makrophagen, also auch die dadurch hervorgerufene Entzündung hemmt. Der CFH Polymorphismus H402 führt zu einer drastisch reduzierten Bindung von CFH an MDA. Träger dieses Polymorphismus' haben ein stark erhöhtes Risiko an AMD zu erkranken, was einen kausalen Zusammenhang zwischen MDA-Bindung und AMD-Pathogenese nahelegt. Diese Entdeckungen tragen zu einem besseren Verständnis der

Immunantwort auf oxidativen Stress bei, was zu verbesserter Prävention und Therapie von AMD und anderen chronisch-entzündlichen Erkrankungen führen wird.

## 2. INTRODUCTION

Oxidative stress is caused by an imbalance between the production of reactive oxygen species and the organism's ability to detoxify the reactive intermediates. It has been implicated in the pathogenesis of many different diseases, including atherosclerosis, age-related macular degeneration (AMD), rheumatoid arthritis, acute lung injury, Alzheimer's disease, and Parkinson's disease <sup>1</sup>.

### 2.1 Sterile inflammation and danger-associated molecular patterns

Inflammation is a crucial mechanism during host defense against invading pathogens. Microbial infections trigger a cascade of signals that lead to the recruitment of innate immune cells such as neutrophils and macrophages. These phagocytes clear infectious microorganisms and eventually lead to the activation of adaptive immune responses via lymphocytes. Similar to the eradication of pathogens, the inflammatory response is also crucial for tissue and wound repair. Inflammation as a result of trauma, ischaemia–reperfusion injury, or chemically induced injury, has been termed “sterile inflammation”, as it typically occurs in the absence of infectious agents. Nevertheless, sterile inflammation shares many features with inflammation caused by microbial infections, including the recruitment of neutrophils and macrophages to the site of tissue injury and the production of pro-inflammatory cytokines and chemokines.

Despite its important role in pathogen clearance and tissue repair, inflammation can be detrimental to the host when it is not resolved and becomes chronic. Examples of sterile inflammatory diseases include Alzheimer's disease, where activated microglial cells adjacent to  $\beta$ -amyloid-containing plaques contribute to disease, and ischaemia–reperfusion injury, where the restoration of blood flow after an ischemic period causes further tissue destruction as a result of inflammatory responses at the site of injury <sup>2,3</sup>. Sterile inflammation is also an important component of atherosclerosis and tumor formation <sup>4,5</sup>.

Several classes of germline-encoded receptors are important for sensing microorganisms and for the subsequent induction of pro-inflammatory responses <sup>6</sup>. These

have been collectively termed pattern recognition receptors (PRRs). They recognize conserved structural moieties that are present on the surface of microorganisms and are therefore often referred to as pathogen-associated molecular patterns (PAMPs). It is now evident that PRRs also recognize non-infectious molecules, which are usually released after tissue damage, and have therefore been termed danger-associated molecular patterns (DAMPs), as they can activate pro-inflammatory pathways similar to PAMPs. DAMPs are endogenous factors that are – under physiological conditions – immediately scavenged. However, under conditions of cellular stress or injury, these molecules can be exposed and trigger excessive inflammation under sterile conditions <sup>6</sup>.

## **2.2 Oxidation-specific epitopes are targets of innate immunity**

During oxidative stress, accumulating free radicals promote the peroxidation of lipids, e.g. in cell membranes, thereby leading to the generation of malondialdehyde (MDA), 4-hydroxynonenal (4-HNE), acetaldehyde and other reactive decomposition products <sup>7</sup>. These can modify endogenous molecules, like proteins, lipids or even DNA, generating novel "oxidation-specific epitopes", which are also present on the surface of apoptotic cells and the apoptotic blebs released from them <sup>8</sup>. Many of these oxidation-derived moieties have been shown to induce pro-inflammatory responses *in vitro* and *in vivo* <sup>9</sup>, and are recognized as DAMPs by innate immune receptors (Fig. 1) <sup>10</sup>. For example, phosphocholine (PC) which is exposed on oxidized, but not on native phospholipids, is bound by the macrophage scavenger receptor CD36 <sup>11-13</sup>, the acute phase reactant C-reactive protein (CRP) <sup>14</sup>, and the murine natural IgM antibody EO6/T15 <sup>15, 16</sup>. All these represent germline encoded receptors, suggesting an evolutionary selection against oxidation derived neopeptides as important targets of innate immunity.

PC represents only one example for such epitopes. However, all of them may potentially serve as ligands for innate immune receptors. Following this hypothesis, Chou et al. recently analyzed the repertoire of natural IgM antibodies with respect to various other "oxidation specific epitopes" and found them to be major targets of innate natural antibodies (NABs) in mice and humans <sup>17</sup>. Of great interest, ~15% of all IgM NABs bound MDA-type adducts, suggesting a great need to defend against this specific modification. MDA and its many condensation products are reliable markers for oxidative stress and have been

associated with many disorders, including atherosclerosis, Alzheimer's disease, multiple sclerosis, acute lung injury, alcoholic hepatitis and diabetic disorders <sup>16, 18-22</sup>. Moreover, MDA-modified proteins are recognized by macrophages and have been found to induce a number of inflammatory responses <sup>23</sup>. Thus, in analogy to PC of oxidized phospholipids, MDA is also recognized by macrophage receptors as well as germline encoded natural IgM antibodies <sup>13</sup>. Given this and the ubiquitous presence of MDA-type adducts in vivo, I hypothesized that - in parallel to the PC-binding plasma protein CRP - another innate plasma protein with specificity for MDA exists. The interaction of such an MDA-binding protein with MDA should have important functional consequences in atherosclerosis and other inflammatory responses that are replete of products of oxidative stress.

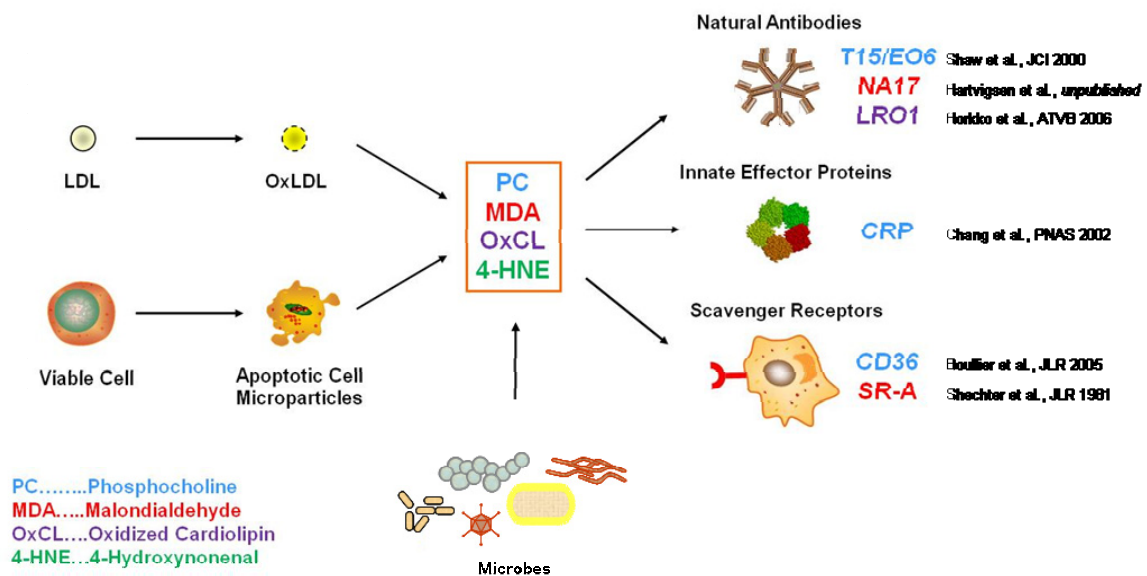


**Fig. 1: Oxidation specific epitopes are targets of innate immunity**

Oxidation specific epitopes like adducts formed by phosphocholine (PC)-carrying oxidized phospholipids, malondialdehyde (MDA), oxidized cardiolipin (OxCL) and 4-hydroxynonenal (4-HNE) are present on oxidized LDL as well as on the surface of apoptotic cells and microparticles shed by them. They are recognized by the innate immune system via natural antibodies, innate effector proteins and macrophage scavenger receptors. In many cases, molecular mimicry exists between oxidation-specific epitopes of self-antigens and epitopes found on microbes.

## 2.3 Generation of Malondialdehyde-adducts

Unlike the short-lived free radicals, aldehydes are relatively stable and also modify targets distant from the initial oxidizing event. Esterbauer et al. have therefore suggested, that reactive aldehydes derived from lipid peroxidation serve as “second toxic messengers” of oxidative stress<sup>7</sup>. MDA mainly occurs as a degradation product of polyunsaturated fatty acids (PUFAs) containing more than two methylene-interrupted double bonds. In mammalian tissue these are represented by arachidonic acid (20:4) and docosahexaenoic acid (22:6). MDA can also be formed from prostaglandin-substrates in an enzymatic process involving platelet thromboxane synthase<sup>24</sup>.

At neutral and alkaline conditions, MDA forms predominantly the enolate anion, which is of low reactivity. The reactivity increases at lower pH when the  $\beta$ -hydroxyacrolein becomes the predominant species. In this state, MDA rapidly forms Michael type 1,4-additions with nucleophilic functional groups like primary amines. MDA can form several different adducts on  $\epsilon$ -aminogroups (Fig. 2). Importantly, MDA and monofunctional aldehydes such as acetaldehyde have been shown to mutually enhance each other's reactivity towards primary amines<sup>25</sup>, which results in the formation of hybrid adducts, the so called malonacetaldehyde (MAA) adducts. These consist of two different modifications: One adduct is a 1:1 adduct of MDA and acetaldehyde and was identified as the 2-formyl-3-(alkylamino)butanal derivative of an amino group (FAAB adduct). The second adduct is composed of two molecules of MDA and one molecule of acetaldehyde and was identified as the 4-methyl-1,4-dihydropyridine-3,5-dicarbaldehyde derivative of an amino group (MDHDC adduct). The generation of the MDHDC-adducts seems to require, in a first step, the formation of the FAAB product, and, in a second step, the generation of an MDA-enamine. The FAAB-moiety is transferred to the nitrogen of the MDA-enamine, forming the circular MDHDC adduct (Fig. 2C)<sup>26,27</sup>.

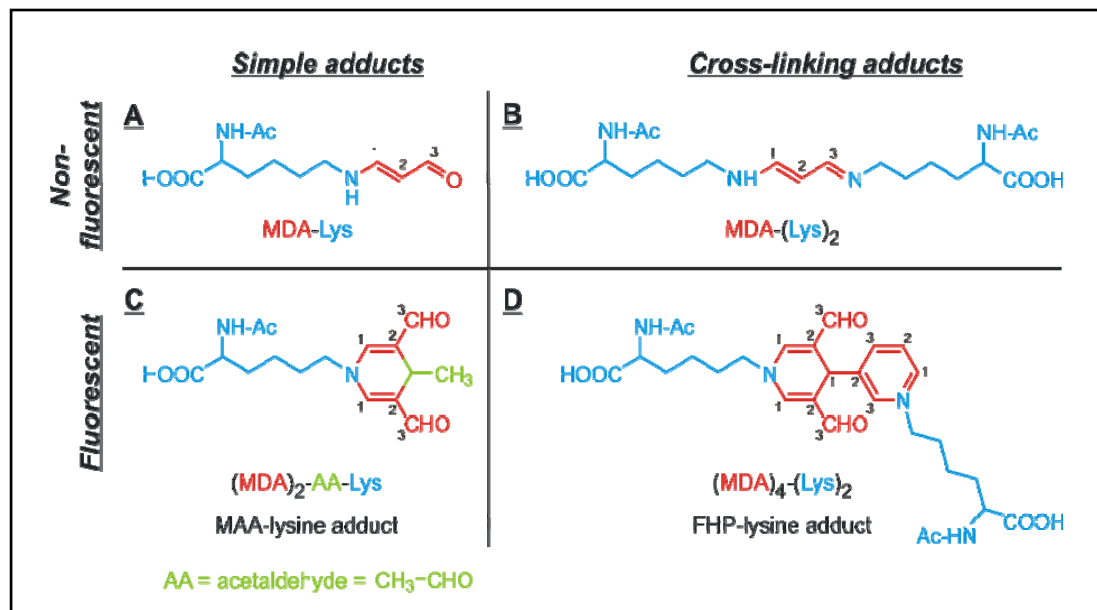


**Fig. 2: MDA-type adducts**

MDA has the potential to generate a variety of different adducts on a carrier molecule. The MAA-modification used in this manuscript is enriched for the MDHDC adduct shown in (C) (*Fig. courtesy of K. Hartvigsen*).

## 2.4 Age-related macular degeneration

The pathogenesis of AMD, a degenerative disorder affecting the retina that leads to irreversible vision loss, has been linked to increased oxidative stress<sup>28, 29</sup>. A hallmark of developing AMD is the accumulation of extracellular deposits, termed drusen, which have been shown to contain MDA<sup>30</sup>.

Age-related macular degeneration is the leading cause of irreversible blindness in older adults in industrialized countries<sup>31, 32</sup>. The overall prevalence of advanced AMD has been projected to increase by more than 50% by the year 2020<sup>33</sup>. The macula is the central portion of the retina, which contains the highest concentration of photoreceptors. It is responsible for central high-resolution visual acuity, and therefore important for reading and recognizing faces. The blood-ocular barrier is maintained by the retinal pigment epithelium (RPE) and the Bruch's membrane. The RPE, immediately posterior to the photoreceptors, has several functions, including phagocytosis of damaged photoreceptors, nutrient transport, and cytokine secretion. The Bruch's membrane is a semipermeable exchange barrier that separates the retinal pigment epithelium from the underlying choroid, the vascular layer of the eye

maintaining blood supply to the outer retina <sup>34</sup>. In aging eyes, focal deposition of acellular, polymorphous debris between the retinal pigment epithelium and Bruch's membrane can occur. These pale, yellowish lesions are called drusen and may be found in both the macula as well as in the peripheral retina. They usually represent the first clinical sign of AMD. However, they are ubiquitous in elderly people and considered a part of normal aging. The presence of only few drusen does therefore not necessarily entail a diagnosis of AMD. Excess drusen, however, can lead to damage to the retinal pigment epithelium, which causes the development of large atrophic areas in the retina (called geographic atrophy), the secretion of angiogenic cytokines such as vascular endothelial growth factor (VEGF), or both <sup>35</sup>.

The Age-related Eye Disease Study defines three different stages during AMD development: Early, intermediate and late AMD, where the latter is further divided into non-neovascular (dry) or neovascular (wet) AMD <sup>36</sup>. Early AMD is diagnosed when less than 20 medium-size drusen (63-124 $\mu$ m diameter) or retinal pigmentary abnormalities are detected. Intermediate AMD is characterized by at least one large druse (>124 $\mu$ m diameter), numerous medium-size drusen (more than 20), or geographic atrophy that does not extend to the center of the macula. Advanced age-related macular degeneration can be either non-neovascular (dry, atrophic, or nonexudative) or neovascular (wet or exudative) and is characterized by drusen and geographic atrophy extending to the center of the macula. In addition, advanced neovascular AMD displays choroidal neovascularization <sup>34, 36</sup>. Importantly, although representing only 10 to 15% of the overall prevalence, neovascular AMD is responsible for more than 80% of legally blind cases resulting from AMD <sup>37</sup>.

Several risk factors increase the susceptibility to AMD. Apart from advanced age, these include environmental factors like smoking as well as genetic factors <sup>32</sup>. In 2005, several independent research groups reported that the polymorphism rs1061170 in the complement factor H (CFH) gene substantially increases the risk for developing AMD <sup>37-40</sup>. In addition, polymorphisms in complement factor B and C2 have been linked to AMD development. Taken together, variations in complement genes may account for approximately 75% of all AMD cases, demonstrating a major role of the complement system in AMD development <sup>41</sup>.

## 2.5 Complement system

The innate immune system provides a rapid and efficient defence against pathogens in most metazoans. However, unlike the adaptive immune system, its effectors are germ line encoded and therefore not able to confer protective immunity. In vertebrates, innate immunity is represented on the one hand by humoral factors like the complement system or natural antibodies (NAbs), and on the other hand by phagocytes and natural killer cells (NK-cells).

The complement system represents an evolutionary old defense mechanism that can be found also in non-vertebrate organisms like arthropods. It is represented by a number of proteins that can be proteolytically cleaved in a cascade ultimately leading to pathogen lysis. The complement components in plasma are mainly synthesized by liver hepatocytes. In addition, they can be locally produced by macrophages and certain epithelial cells. The complement system can be activated by three pathways, all of them leading to the generation of analogue variants of the protease C3-convertase. The classical complement pathway typically requires antigen-antibody complexes as triggers, whereas the alternative and mannose-binding lectin (MBL) pathways can be activated by spontaneous C3 hydrolysis or MBL/ficolin antigens without the presence of antibodies, respectively. In all three pathways, a C3-convertase assembles that cleaves complement component 3 (C3) into C3a and C3b, which then causes a cascade of further cleavage events. Apart from triggering the assembly of the C3- and later the C5-convertases, C3b deposition on surfaces also facilitates the internalization of opsonized cells by phagocytes. Both C3a and C5a have anaphylatoxin activity, which means that they are able to directly trigger degranulation of mast cells as well as to increase vascular permeability and smooth muscle contraction. In addition, C5a is an important chemotactic protein that leads to the recruitment of inflammatory cells. The deposition of the C5b fragment on surfaces sets off the formation of the membrane attack complex (MAC), consisting of C5b, C6, C7, C8, and polymeric C9. MAC is the cytolytic endproduct of the complement cascade; it forms a transmembrane channel, which causes osmotic lysis of the target cell.

## 2.6 Complement Factor H

Complement factor H is the major inhibitor of the alternative pathway of complement activation. As most of the other complement components, this abundant plasma glycoprotein is constitutively secreted by the liver, but is also produced locally by a variety of cell types including retinal pigment epithelial cells, endothelial cells, epithelial cells, platelets, and mesenchymal stem cells<sup>6, 42-45</sup>. The plasma concentration of CFH depends on genetic and environmental factors and varies widely between 116 to 562 µg/ml<sup>46-48</sup>. CFH inhibits the alternative pathway of complement activation in two ways: First, CFH acts as a cofactor for factor I-mediated inhibitory cleavage of C3b. Second, CFH competes with factor B for the binding of deposited C3b, thereby accelerating the decay of the alternative pathway C3 convertase<sup>48-51</sup>. CFH is composed of 20 short consensus repeat (SCR) domains. The N-terminal four SCR domains are responsible for its complement regulatory activities, i.e. the decay accelerating and cofactor activity<sup>52</sup>. The C-terminal domains (SCR18-20) include binding sites for several host factors including C3b, C3d, heparin and cell surface glycosaminoglycans, as well as for microbial virulence factors<sup>53</sup>. On top of this, the C-terminus mediates surface binding of CFH<sup>54</sup>. Once triggered, the alternative pathway of complement can amplify on any surface that is not protected by complement regulatory proteins. Factor H is essential in this as it detects and binds to initial C3b deposits in combination with specific markers on host cells. In fact, CFH binds to C3b on host cells with a 10-fold higher affinity than to C3b deposited on other surfaces<sup>55</sup>. This reverse recognition is essential, as it prevents alternative pathway activation on host cells while allowing it to proceed on foreign surfaces<sup>56-58</sup>. The human host markers bound by CFH are assumed to be polyanionic molecules, such as highly sulfated heparin and glycosaminoglycan (GAG) chains of proteoglycans<sup>59, 60</sup>.

Besides inhibiting complement activation on certain surfaces, CFH plays an important regulatory role also in the fluid phase by preventing complement activation following spontaneous C3 hydrolysis. In the absence of CFH, spontaneous complement activation in plasma leads to the consumption of the complement components C3 as well as factor B, which manifests in severe kidney diseases like membranoproliferative glomerulonephritis (MPGN)<sup>49</sup>.

The CFHL1 protein, which is derived from the *CFH* gene by means of alternative splicing, is composed of the seven N-terminal domains of CFH and has a unique C-terminal

four amino acids extension. Consequently, CFHL1 shares ligand binding and complement regulatory activity with the N terminus of CFH<sup>61</sup>.

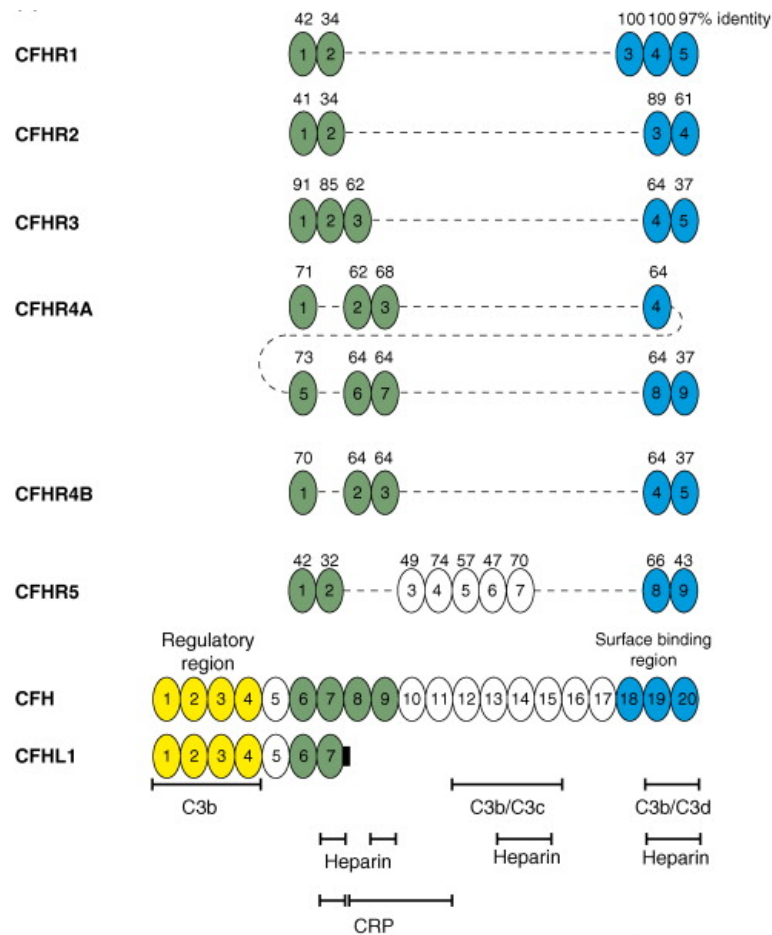


**Fig. 3: The human complement Factor H protein family**

For the CFH and the CFHR4 genes, two splice variants encode related proteins (CFH and CFHL1; CFHR4A and CFHR4B). All CFHRs contain domains homologous to the C-terminal surface and ligand recognition region (SCRs 19–20) and to the middle region (SCRs 6–9) of CFH. CFHR proteins lack SCRs related to the complement regulatory domains (SCRs 1–4) of CFH. For CFH, the localization of binding domains for C3b and its fragments, as well as for heparin and C-reactive protein (CRP), are indicated (Fig. adapted from Joszi & Zipfel, *Trends Immunol* 2008<sup>62</sup>).

Furthermore, the CFH gene family encodes for 5 CFH-related proteins (CFHR1-5), which consist of four to nine SCR domains (Fig. 3). The N-terminal SCRs of all five CFHR proteins show high sequence homology to SCRs 6–9 of CFH. Similarly, the C-termini of all CFHRs are homologous to the C-terminal surface binding region of CFH. All CFHRs lack cofactor activity as well as decay accelerating activity<sup>63,64</sup>.

Using an unbiased proteomic approach I identified complement factor H as the major plasma binding protein for MDA. I show that CFH has the capacity to inhibit binding of MDA-modified LDL (MDA-LDL) to macrophages and to neutralize MDA-induced inflammatory responses *in vitro* and *in vivo*. A common polymorphism in *CFH* associated with AMD dramatically disrupts the ability of CFH to bind MDA. My data directly link oxidative stress with the AMD associated CFH variant and suggest that the ability of CFH to bind MDA is critically involved in inflammatory diseases such as AMD and atherosclerosis.

### **3. AIM OF THE STUDY**

MDA adducts appear to be one of the most prominent products of oxidative damage and accumulate in a variety of different diseases. Elucidating the molecular mechanisms by which oxidative damage challenges the immune system will eventually pave the road for novel diagnostic and therapeutic approaches in multiple pathologies. It is the aim of this thesis to identify novel interactors of MDA in human plasma and to investigate the role of this interaction in health and disease.

## 4. METHODS

### 4.1 Subjects and Clinical Diagnosis

112 patients with a clinical diagnosis of AMD and 67 control subjects of similar age, gender and smoking habits, who showed no signs of macular disease were studied <sup>65</sup>. The mean age of the AMD patient cohort was 75.6 years (SD, 6.6; range, 59-94) and that of the controls was 70.1 years (SD, 6.0; range, 60-86). Within the patient and control cohort, 53% and 52%, respectively, were non-smokers; 38% and 39%, respectively, were ex-smokers; and 9% and 9%, respectively, were current smokers.

Within the AMD cohort, 78 (70%) had choroidal neovascularization (CNV), 25 (22%) had geographic atrophy (GA), and 9 (8%) had early AMD. Digital fundus photographs were obtained from all participants. In patients with CNV, optical coherence tomography and fluorescein angiography were performed. Fundus autofluorescence imaging was performed in patients with GA. All fundus images were graded separately by two independent readers (HPNS and PCI) according to the classification system of the International ARM Epidemiological Study Group <sup>66</sup>.

All subjects were of Caucasian descent and were recruited within the same time period. Subjects were characterized by means of a standardized case report form, which included smoking history, a comprehensive medical history and current medications. Subjects were excluded if they suffered from diseases known to cause abnormal complement levels. Informed consent was obtained from all subjects.

For immunohistochemistry, globes from 49-93 year old donors were obtained from the National Disease Research Interchange (NDRI, Philadelphia, PA) within 6 hours of death, who were on life support for < 24 hours (Table 1). Macular calottes were fixed for 1 h in 2% paraformaldehyde and then cryoprotected by progressive infiltration in 10% and 20% sucrose in PBS (w/v) before freezing in 2:1 sucrose 20% (w/v):OCT compound at -80 °C.

**Table 1: Patient description**

Donor	Age	Gender	D-E (hr)	AMD	Cause of Death	rs1061170
1	49	M	3:45	No	Trauma	tt
2	72	F	6:00	No	Cardiac arrest	ct
3	70	F	6:10	Yes	Lung cancer	ct
4	85	F	2:30	Yes	Multiorgan system failure	tt
5	74	M	2:40	Yes	Brain cancer	ct
6	90	F	3:53	Yes	Congestive heart failure	cc
7	93	F	5:45	Yes	Renal Failure	cc

Atherectomy material was collected during percutaneous coronary intervention through catheter aspiration and immediately fixed in EDTA/BHT/paraformaldehyde. Subsequently, the fixed specimens were embedded in paraffin and sections prepared for immunohistochemistry.

The research protocols were in keeping with the provisions of the Declaration of Helsinki, and approval was obtained from the local Ethics Review Board at the University of Bonn and University of California San Diego, respectively.

## 4.2 Plasma Samples

Venous blood was collected from all subjects into tubes containing dipotassium EDTA at a final concentration of 8 mM. The plasma was separated from blood cells by centrifugation (20 min/1,000 x g) within 3 hours after venipuncture and frozen in aliquots at -80°C until analysis. All subjects had normal creatinine and cystatin C values, and the two subject groups were not significantly different for these variables. CFH levels in plasma were measured as previously described<sup>67</sup>.

### **4.3 Genotyping**

Genomic DNA was extracted from peripheral blood leukocytes following established protocols. Genotyping was done by TaqMan SNP Genotyping or by direct sequencing of SNPs. TaqMan Pre-Designed SNP Genotyping Assays (Applied Biosystems, Foster City, U.S.A.) were performed according to the manufacturer's instructions and were analyzed with a 7900HT Fast Real-Time PCR System (Applied Biosystems). Direct sequencing was performed with the Big Dye Terminator Cycle Sequencing Kit Version 1.1 (Applied Biosystems) according to the manufacturer's instructions. Reactions were analyzed with an ABI Prism Model 3130xl Sequencer (Applied Biosystems). Individual genotypes that were ambiguous or missing were reanalyzed resulting in a call-rate of 100% for all SNPs tested <sup>65</sup>. Genetic associations with CFH binding to coated MDA-LDL binding were assessed using PLINK version 1.07 <sup>68</sup>.

When DNA was extracted from histological specimen, QIAamp FFPE Tissue Kit (Qiagen) was used. Genotyping was performed in the Molecular Diagnostic Laboratory of the Medical University of Vienna using a certified kit.

### **4.4 Intravitreal injection**

C57BL/6 mice were anesthetized and the pupils dilated. Using a dissecting microscope, intravitreal injections into one eye of each mouse (n=5 per group) were performed with a pump microinjection apparatus (Harvard Apparatus, Holliston, MA) and a glass micropipette that was calibrated to deliver 1  $\mu$ l of vehicle containing either BSA (2.34  $\mu$ g), MAA-BSA (2.34  $\mu$ g), CFH (2.2 $\mu$ g), or a combination of CFH and BSA-MAA(4.4 $\mu$ g of CFH and 2.4  $\mu$ g of BSA-MAA) pre-incubated for 1 hour, on depression of the foot switch. Six hours later, mice were sacrificed, eyes were enucleated, and the RPE/choroid was dissected.

Total RNA was extracted from RPE/choroid and retina using the Qiagen RNeasy mini kit (Qiagen, Valencia,CA) and reversely transcribed using the high capacity RNA to cDNA kit (Applied Biosystems) according to the manufacturer's protocol. To demonstrate the presence of RPE in the RPE/choroid extract, the expression of RPE65 in the RPE/choroid samples was determined by conventional RT-PCR. Samples were also tested for Rhodopsin,

a photoreceptor marker. The primer sequences are listed in Table 2. The following PCR parameters were used: 95°C for 5 minutes, follow by 35 cycles of 95°C for 30 sec, 60°C for 30 sec, and 72°C for 1 min, and 72°C for 5 minutes at the end of the reaction. The product was run on a 2% Agarose gel.

## 4.5 Proteins and antibodies

Full length CFH was purchased from Calbiochem or CompTech. CFH derived from genotyped AMD patients was purified from plasma as described <sup>69</sup>. Briefly, patient plasma was diluted in Sterofundin (Braun, Melsungen, Germany) and applied to a HiTrap Heparin HP column (GE Healthcare, Freiburg, Germany). After loading, the column was washed extensively and bound protein was eluted using 30% Sterofundin supplemented with 1M NaCl. The eluted fractions were assayed for the presence of CFH, and the positive fractions were combined, desalted and adjusted to 25mM Tris pH 8.0. The desalted sample was applied to anion exchange chromatography using a MONO Q 4.6/100 PE column (GE Healthcare). Bound proteins were eluted with a linear gradient of 30% 25mM Tris, 1M NaCl pH 8.0 and the CFH containing elute fractions were combined, concentrated and dialyzed against DPBS (Lonza, Verviers, Belgium). Recombinantly expressed FHL1 as well as the CFH deletion constructs were prepared in the pBSV-8His baculovirus expression system as previously described <sup>69</sup>. In brief, *Spodoptera frugiperda* (Sf9) cells were grown in monolayers at 27°C and infected with the corresponding recombinant virus of each deletion construct using a multiplicity of infection of five. One week after infection, the culture supernatant was harvested and the recombinant constructs were purified by nickel affinity chromatography. Each protein was concentrated and dialyzed against DPBS (Lonza). Human LDL was isolated from EDTA-plasma of healthy donors after overnight fasting by differential density ultracentrifugation on OTD Combi (Sorvall) over the density range of  $\rho$  1.019 to 1.063 g/ml as described <sup>70</sup>. The quality of LDL-preparations was checked by lipoprotein electrophoresis and protein content was measured by the Lowry method. LDL was sterile filtered and stored at 4°C. Copper sulfate-oxidized LDL (CuOx-LDL) and MDA-LDL were prepared as described previously <sup>70</sup>. The MAA-modifications of LDL, BSA (SigmaAldrich) or polylysine (1-4kD, SigmaAldrich) were performed as described previously <sup>27</sup>. Briefly, protein was adjusted to 2mg/ml and modified by reacting with 0.1M MDA in the presence of 0.2M acetaldehyde in phosphate buffered saline at pH 4.8 for 3.5h at 37°C.

Unbound MDA and acetaldehyde were removed by dialysis against PBS and the degree of modification was assessed by the TNBS-test <sup>71</sup> as well as by the amount of specific MAA fluorescence present ( $\lambda_{\text{max. excitation}}$  394 nm/ $\lambda_{\text{max. emission}}$  462 nm). To generate 4-HNE-BSA, 2mg of BSA were modified with 5 $\mu$ mol 4-HNE (Alexis biochemicals) in PBS pH 9 for 24h at 37°C. Reducing conditions were maintained by adding 20mM CNBH<sub>3</sub> to the reaction. Unbound entities were removed by dialysis against PBS pH 7.4. Modification was verified by the TNBS-assay, as well as by immunoassay using the 4-HNE reactive antibody NA59 <sup>72</sup>. CEP-BSA was a kind gift from Dr. John W. Crabb (Cleveland Clinic) <sup>73</sup>. Biotinylated proteins were generated with EZ-Link SulfoNHS-biotin (Pierce) according to the manufacturer's instructions. Protein concentrations were determined by Lowry or BCA-method according to the manufacturer's instructions (Pierce).

MDA2 is a murine IgG monoclonal antibody <sup>74</sup>, and EO14 a murine IgM NAb <sup>16</sup> that bind to malondialdehyde (MDA)-lysine epitopes present on modified LDL or other MDA-modified proteins but not to native LDL or unmodified proteins. EO6 is a murine IgM NAb that binds to the PC head group of oxidized, but not native, phospholipids as described <sup>16</sup>. All antibodies were purified with high performance liquid chromatography. Apolipoprotein (apo) B-100 specific monoclonal antibodies MB47 <sup>75</sup> and MB24 <sup>76</sup> (both IgG2a) against human apoB-100 were purified by protein A chromatography. Anti-human CFH antiserum and anti-mouse CFH mAb were purchased from Calbiochem and SantaCruz, respectively. In addition, human recombinant CFH (Calbiochem) was used to generate a monospecific anti-CFH antisera in guinea pigs. The IgG was purified with protein A and biotinylated according to the manufacturer's instructions (Pierce) for use in assays to detect the ability of plasma CFH to bind to MDA as described below. The murine IgG2a isotype control antibody was purchased from Beckton Dickinson.

## 4.6 Bead coupling and pulldown-procedure

Unmodified or MDA-modified polylysine was coupled to NHS-activated sepharose (GE Healthcare) according to the manufacturer's instructions. Plasmas obtained from LDLR<sup>-/-</sup>RAG<sup>-/-</sup> mice or human donors were diluted to a concentration of 1 mg/ml total protein. To minimize the amount of proteins binding to unmodified polylysine, plasma dilutions were incubated with polylysine-coupled beads for 2h at 4°C. After the incubation, supernatant was

incubated with either polylysine- or MAA-polylysine-beads for another 2h at 4°C. Beads were washed 3 times with TBS (pH 7.4, 500mM NaCl, 0.5% NP-40, 2mM CaCl<sub>2</sub>, 1mM MgCl<sub>2</sub>). After the last wash, bound proteins were dissociated by adding LDS-sample buffer (Invitrogen) and heating at 95°C for 5min. The supernatants were used for further analysis.

The samples were separated by one-dimensional sodium dodecyl sulfate polyacrylamide gel electrophoresis (SDS-PAGE), digested *in situ* with trypsin and analyzed by LC-MSMS on a quadrupole time-of-flight (QTOF Premier) mass spectrometer (Waters, Manchester, UK) coupled to a 1100 series nano-HPLC system (Agilent Technologies, Palo Alto, CA). Obtained data was searched against the IPI\_MOUSE database v.3.32 appended with known contaminants (e.g. trypsin, human keratin proteins).

#### **4.7 Immunoblotting**

The samples were separated by gradient SDS-PAGE (Invitrogen) and blotted on PVDF-membranes (Whatman, Fig. 4) or nitrocellulose-membranes (Whatman, Fig. 11). Membranes were blocked in 5% non-fat dry milk in PBS with 0.05% Tween 20. Following 3 washing steps, blots were probed for the presence of CFH using goat polyclonal anti-human-CFH (Calbiochem, diluted 1:10,000 in 1% non-fat dry milk in PBS with 0.05% Tween 20 (antibody diluent)) or goat polyclonal anti-mouse-CFH (SantaCruz, diluted 1:1,000 in antibody diluent). Blots with samples from the co-factor assay were probed for iC3b using goat polyclonal anti-human-C3 (Comptech) diluted 1:2,000 in antibody diluent. Anti-goat-IgG conjugated to horseradish peroxidase (Calbiochem, diluted 1:5,000 in antibody diluent) was used as a secondary antibody.

#### **4.8 Immunoassay**

Chemiluminescent ELISA was performed as previously described<sup>70</sup>. Washing steps were performed on microplate washer ELx405 (BioTek). In brief, antigens at concentrations of 1-5µg/ml in PBS containing 0.27mM EDTA were added to each well of a 96-well white, round bottom microtitration plate (Thermo, MicrofluorII roundbottom) and incubated 1h at 37°C. After washing and blocking steps, plates were incubated with purified CFH or CFH

fragments at a concentration of 1-5µg/ml in TBS-BSA (TBS pH 7.4, containing 1% BSA) overnight at 4°C. Bound CFH or CFH fragments were detected with goat polyclonal anti-human-CFH (Calbiochem, 1:10,000 in TBS-BSA) and mouse anti-goat-IgG conjugated to alkaline phosphatase (AP) (SigmaAldrich, 1:30,000 in TBS-BSA). In reciprocal experiments, CFH or fragments were coated and binding of biotinylated MAA-BSA was determined. Separate experiments demonstrated the ability of polyclonal anti-human CFH to recognize all CFH fragments (data not shown). When determining potential binding of C3 (Comptech) and CRP (Calbiochem) to MAA-BSA, the purified proteins were used at a concentration of 5µg/ml and detected with either goat polyclonal anti-human C3 (Comptech, 1:4,000) or goat polyclonal anti-human CRP (SigmaAldrich, 1:10,000). For immunoassays including CRP, blocking, dilution and washing buffer contained 2mM CaCl<sub>2</sub> 1mM MgCl<sub>2</sub> because many interactions of CRP, including its binding to the PC-headgroup, have been described as being dependent on bivalent cations<sup>14</sup>.

To determine the ability of CFH in human plasma to bind to MDA-LDL or MAA-BSA, human plasma from subjects with known genotypes for the 402 polymorphism was added at varying dilutions to microtiter wells containing either coated MDA-LDL or MAA-BSA. Samples were diluted in TBS-BSA and incubated for 1 hr at room temperature. After extensive washing with a microtiter plate washer, the bound CFH was detected with biotinylated guinea pig anti-human CFH followed by AP-conjugated NeutrAvidin (PerkinElmer, 1:10,000 in TBS-BSA). AP-conjugated secondary reagents were detected using Lumiphos (Lumigen, 50% solution in water) and a Dynex Luminometer (Dynex Technologies) and results expressed as relative light units (RLU) per 100ms.

#### **4.9 Competition immunoassay**

Competition assays were performed by chemiluminescent ELISA in which either binding of biotinylated MAA-BSA to coated CFH or binding of CFH (purified or in whole human plasma) to coated MAA-BSA was competed by native LDL, MDA-LDL, MAA-LDL, CuOx-LDL, BSA or MAA-BSA. Purified CFH or MAA-BSA were coated at a concentration of 2µg/ml or 0.5-1µg/ml, respectively. Biotin-labeled MDA-LDL or CFH at a concentration of 0.5µg/ml or 1µg/ml or human plasma at a dilution of 1:2,000 (in TBS-BSA) were mixed with indicated concentrations of unlabeled native LDL, MDA-LDL, MAA-LDL or CuOx-

LDL and added to coated wells overnight at 4°C. Bound biotin-MDA-LDL was detected with AP-conjugated NeutrAvidin (PerkinElmer, 1:10,000 in TBS-BSA). Bound CFH was detected with goat polyclonal anti-human-CFH (Calbiochem, 1:10,000 in TBS-BSA) and AP-conjugated mouse anti-goat-IgG (SigmaAldrich, 1:30,000 in TBS-BSA). Substrate was added and luminescence was measured as described above. To express the relative binding affinities, the dissociation constants ( $K_d$ ) were determined according to the Klotz method <sup>77</sup>. Calculations are based on the concentration of competitor at which binding was inhibited by 50%.

#### **4.10 Immunohistochemistry and confocal microscopy**

Cryosections were blocked with 2% normal goat serum and an avidin-biotin complex (ABC) blocking kit (Vector Laboratories, Inc., Burlingame, CA), followed by overnight incubation at 4°C with mouse MDA2 monoclonal antibody (1:2,000) or mouse IgG1, and guinea pig anti-CFH antibody (5µg/ml) or guinea pig IgG, or mouse C3d monoclonal antibody (1:100; AbD Serotec, Inc. Oxford, UK) or mouse IgG1. After incubating for 30 min at room temperature with rat biotinylated secondary antibody (1:4,000; Vector laboratories, Inc.), followed by AP-conjugated streptavidin (1:500; Sigma-Aldrich, Inc. St. Louis, MO), AP activity was visualized with a 5-bromo-4-chloro-3-indoyl phosphate (BCIP)-NBT kit (Vector Laboratories, Inc.).

Paraffin section of atherectomy samples were stained with the antibodies described above following a previously established protocol <sup>17</sup>.

Co-localization of CFH and EO14 was visualized by confocal microscopy. ARPE-19 cells were incubated at 65 °C for 45 min to induce necrosis, then washed in DPBS supplemented with 1 % BSA followed by a 30 min incubation of 10 µg / ml CFH (CompTech). After a washing step monoclonal EO14 and polyclonal CFH antiserum (CompTech) were added, followed by the corresponding anti-mouse FITC (Dako, Hamburg, Germany) or anti-rabbit Alexa 647 (Invitrogen, Karlsruhe, Germany) labeled secondary antibodies. Cells were further stained with DAPI (Sigma-Aldrich) and examined with a laser scanning microscope LSM 510 META (Zeiss, Jena, Germany).

#### **4.11 Microparticle isolation and staining**

Specific cell derived microparticles were obtained from the human T-lymphoma cell line Jurkat. After inducing apoptosis with staurosporine (1nM) for 24h, cells were sedimented and submicron particles were isolated from the supernatant by centrifugation at 16,100g for 30min. The microparticles were washed three times in PBS before staining. CFH at a concentration of 10 $\mu$ g/ml was mixed with BSA or MAA-BSA at a concentration of 472 $\mu$ g/ml and incubated for 30min at 4°C. The washed microparticles were stained either with the competition mix or CFH alone for 30min at 4°C. After washing, bound CFH was detected with goat polyclonal anti-human-CFH (Calbiochem, 1:200 in PBS-BSA) and anti-goat IgG-FITC (Dako, 1:200) on a FACScalibur (BD).

#### **4.12 Co-factor assay**

MAA-BSA at a concentration of 5 $\mu$ g/ml in PBS was bound to the surface of a 96-well flat-bottom microtitration plate (NUNC Maxisorp). After washing and blocking, CFH was bound to coated MAA-BSA at concentrations of 0.2-5 $\mu$ g/ml in PBS-BSA (PBS pH 7.4, containing 1% BSA) for 1h (if not otherwise indicated) at room temperature. If competition was performed, CFH at 5 $\mu$ g/ml was applied as a mixture with CFH18-20 or CFH15-19 at indicated concentrations. Unbound protein was removed by washing and plates were incubated with C3b (Comptech, 0.8 $\mu$ g/ml) and factor I (Comptech, 0.2 $\mu$ g/ml) in PBS for 90min at 37°C. The reaction was stopped by adding LDS-sample buffer (Invitrogen) and samples were denatured at 95°C for 5min. After SDS-PAGE, C3-cleavage products were visualized by immunoblotting.

#### **4.13 Macrophage foam cell assay**

Mouse peritoneal macrophages were isolated from 8-12 weeks old C57BL/6 mice by peritoneal lavage 3 days after the injection of thioglycollate. Macrophages were plated in 96-well plates at 1.5x10<sup>5</sup> cells per well and non-adherent cells were removed after 1 h, the cells were washed twice with RPMI 1640 and macrophage monolayers were cultured overnight in complete medium (RPMI 1640 containing 10% FCS, 2mM L-glutamine, 100 units/ml

penicillin/streptomycin) before use in the foam cell assay. Native LDL or MDA-LDL were diluted to a concentration of 50µg/ml in medium (RPMI 1640 containing 1% BSA). These solutions were added to macrophage-containing wells in the absence or presence of CFH (200µg/ml, Calbiochem) followed by an incubation for 24h at 37°C. Wells were washed two times with RPMI 1640 and cells were fixed by incubating with paraformaldehyde (PBS containing 4% PFA, 4% sucrose) for 1h at room temperature. After fixation, cells were stained with Oil-Red-O as previously described<sup>78</sup>. The number of Oil Red-O positive cells was quantified among at least 500 cells counted and data were presented as percentage of Oil Red-O positive cells.

#### **4.14 Macrophage binding assay**

Binding of biotinylated MAA-LDL to thioglycollate elicited peritoneal macrophages plated in microtiter wells was assessed by a chemiluminescent binding assay as described<sup>70</sup> with modifications. Briefly, isolated human LDL was biotinylated according to the manufacturer's protocol (Cat# 21326; Pierce Biotechnology) prior to MAA modification. The biotinylated MAA-LDL (5 µg/ml) was incubated in the absence or presence of serially diluted CFH or BSA in 1% BSA-PBS. The ligand-competitor solutions were incubated overnight at 4°C. Thioglycollate elicited peritoneal macrophages were cultured in 10% fetal bovine serum in DMEM (DMEM-10) and plated in 100 µl L929-fibroblast conditioned media at 100,000 cells/well in sterile 96-well flat-bottom white plates (Greiner Bio-One) at 37°C. The plating media consisted of 20% L929-fibroblast conditioned DMEM-10 and 80% fresh DMEM-10 and served as a source of growth factors, including macrophage colony-stimulating factor (M-CSF). After 24 hours, plates were washed gently 5 times with PBS using a microtiter plate washer (Dynex Technologies, Chantilly, VA), and wells were blocked with 200 µl of ice-cold 1% BSA-PBS for 30 min, while plates were kept on ice. After washing, macrophages were incubated with ice-cold ligand-competitor solutions (100 µl/well) for 2 hours on ice, washed again, and fixed with ice-cold 3.7% formaldehyde in PBS for 30 min in the dark. After fixing the macrophages, the remainder of the assay was carried out at room temperature. Macrophage-bound biotinylated MAA-LDL was detected as described above. Data were recorded as relative light units counted per 100 milliseconds

(RLU/100ms) and expressed as a ratio of binding in the presence of competitor (B) divided by binding in the absence of competitor ( $B_0$ ).

#### 4.15 Cell stimulations

Human THP-1 monocytic cells were cultured in RPMI-1640 supplemented with 10% FCS. The stimulation medium contained BSA or MAA-BSA at 50 $\mu$ g/ml and/or CFH at 200-12.5 $\mu$ g/ml and was incubated for 30min at RT before plating. Before stimulation, cells were washed with serum-free RPMI-1640 and incubated with the stimulation medium at a density of 5x10<sup>5</sup> cells/ml for 14h. Cells were removed by centrifugation (500g, 10min) and supernatants were assayed for IL-8 by ELISA according to the manufacturer's instructions (BecktonDickinson). For the simulation of THP-1 cells with LPS and phorbol-myristate-acetate (PMA), concentrations of 1 $\mu$ g/ml and 50ng/ml were used, respectively. ARPE-19 retinal pigment epithelial cells were seeded at 1x 10<sup>6</sup> cells/cm<sup>2</sup> and grown in DMEM/F12 (1:1) plus 10% FCS until visually confluent. After serum starvation in DMEM/F12 (1:1) plus 0.1% BSA for 24 h, cells were stimulated with BSA or MAA-BSA at 50 $\mu$ g/ml for 24 hours in DMEM/F12 (1:1) plus 0.1% BSA. Total RNA was isolated from ARPE-19 cells using the RNeasy Mini Kit (Qiagen, Inc. Valencia, CA), and cDNA was generated by using the High Capacity RNA-to-cDNA kit (Applied Biosystems, Inc., Foster City, CA). Gene expression was measured using intron-spanning primer sets (Table 2) or on demand probe sets (Applied Biosystems, Inc.). Human IL12b quantitect primers were ordered from Qiagen. PCR reactions were analyzed by using either the Applied Biosystems 7900 HT Fast Real-time PCR system or Applied Biosystems StepOnePlus Real-time PCR system (Applied Biosystems, Inc.).

Bone-marrow derived macrophages were generated by M-CSF differentiation of bone-marrow cells for 7 days. Purity of >90% was verified by flow cytometry using an antibody directed against the macrophage-marker CD11b (BecktonDickinson) (data not shown). Cells (1.5x10<sup>6</sup> per well) were seeded in a 12-well tissue culture plate. After adherence, cells were washed 2x with PBS and stimulated with the indicated amounts of BSA or MAA-BSA in RPMI for 16h. Supernatants were cleared of cells by centrifugation (500g 10min) and were assayed for KC by ELISA according to the manufacturer's instructions (R&D Systems).

**Table 2: Primers used for RT-qPCR of THP-1 cDNA**

<b>primer designation</b>	<b>primer sequence</b>	<b>product size [bp]</b>
hActin_fw	cgcgagaagatgaccagatc	125
hActin_re	tcaccggagtccatcacga	
hTNFa_fw	cagccttctccttctga	197
hTNFa_re	cagcttgagggttgctaca	
hIL-8_fw	tctgcagctctgtggaagg	229
hIL-8_re	acttctccacaacctctgc	
hIL1b_fw	cagtggcaatgaggatgacttg	117
hIL1b_re	tggagattcgtagctggatg	
mRPE65_fw	gggaagaagttaaagaaatgctatg	96
mRPE65_re	ttctgcctgtgacgacctt	
mRho_fw	tcacgctatcatgggtgtgtctt	190
mRho_re	aggaatggtgaagtggaccacgaa	

#### **4.16 Statistical analysis**

Data are presented as mean±SD or mean±SEM where indicated. Results were analyzed by one-way analysis of variance and Student's unpaired *t* test.

## 5. RESULTS

### 5.1 CFH binds to MDA in mouse and human plasma

I used an unbiased proteomic approach to identify plasma proteins binding to MDA-modifications. Because normal plasma contains high titers of potentially interfering natural antibodies binding to MDA<sup>17</sup>, I purified MDA-binding proteins from plasma isolated from atherosclerotic LDLR<sup>-/-</sup> RAG<sup>-/-</sup> mice that lack immunoglobulins. The LDLR<sup>-/-</sup> background was initially chosen to allow the identification of potentially upregulated acute phase proteins induced during atherogenesis. Pooled plasma was incubated with sepharose-beads coupled to either malondialdehyde-acetaldehyde (MAA)-modified or unmodified polylysine, respectively. MAA is an advanced MDA-lysine adduct whose structure is shown in Fig. 2<sup>27</sup>. Bound proteins were eluted and identified by mass spectrometry. As many as 45 unique peptides were found exclusively in MAA-polylysine pull downs, of which more than 55% could be attributed to CFH (Fig. 4A). Immunoblot analysis of proteins eluted from the beads revealed the presence of CFH on MAA-coated beads but not on control beads. This finding was confirmed in an experiment using human plasma (Fig. 4B-C). Interestingly, the anti-CFH antibody detected additional bands with a lower molecular weight, which may represent factor H related proteins that share high sequence homology with CFH.

### 5.2 CFH interacts directly with MDA-modifications

Using ELISA, I then demonstrated that the interaction of CFH with MDA was direct and occurred independently of the protein carrying the adducts. Purified CFH bound in a calcium-independent manner to both MAA-LDL, as well as to MAA-BSA, but not to unmodified, native BSA or native LDL, respectively (Fig.5A-B). Moreover, I tested binding of CFH to the oxidation specific modifications PC-BSA, which is bound by C reactive protein (CRP), as well as 4-hydroxynonenal-BSA (4-HNE-BSA) and carboxyethylpyrrole-BSA (CEP-BSA). None of these modifications were bound by CFH (Fig. 5C-E). CRP and C3 were also detected in the MAA-polylysine pulldowns (Fig. 4A). I demonstrated that neither bound to coated MAA-BSA (Fig. 5C, Fig. 5F) and thus their presence in the pulldowns was most likely due to indirect binding via CFH.

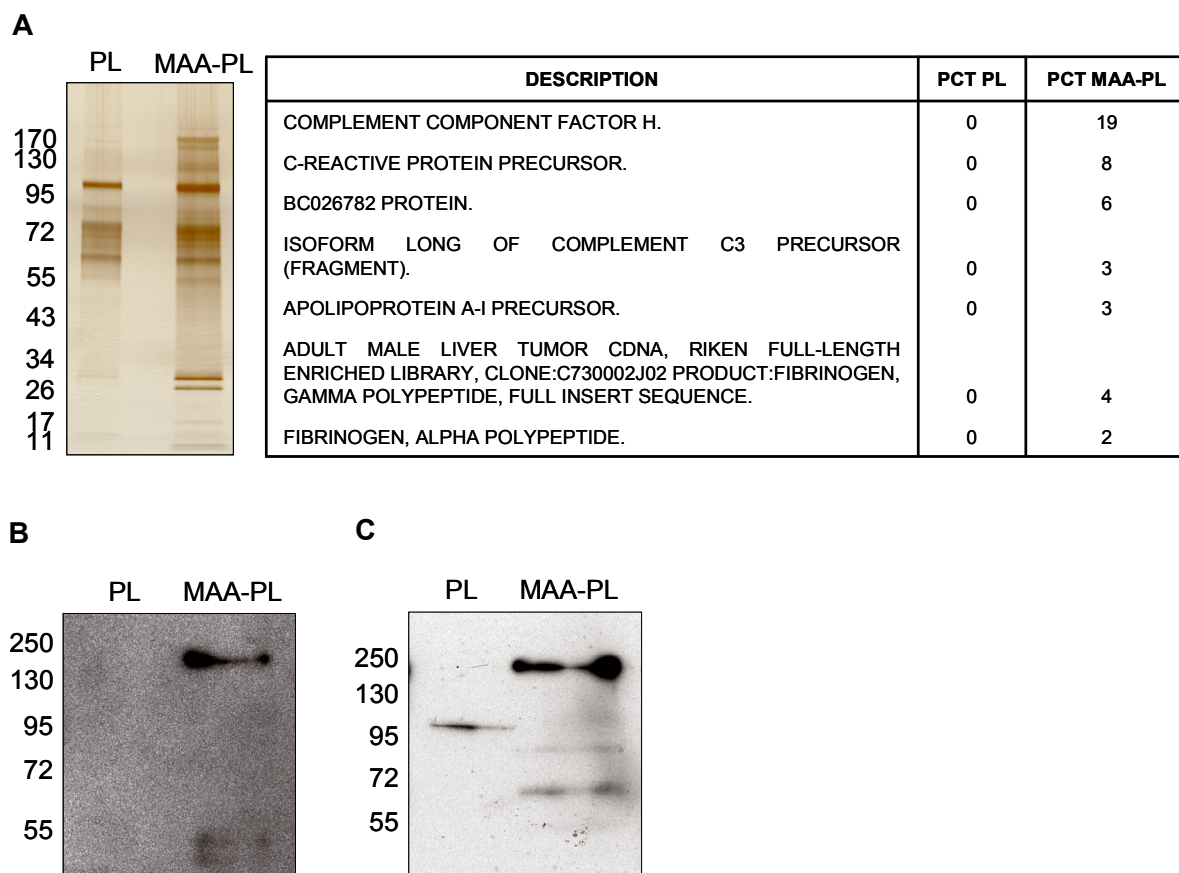


**Fig. 4: Proteomic identification of CFH**

(A) Eluates from either polylysine (PL) or MDA-polylysine (MDA-PL) beads incubated with plasma from LDLR<sup>-/-</sup>/RAG<sup>-/-</sup> mice were separated by one-dimensional SDS-PAGE and the proteins were stained with silver nitrate. Twenty regions were excised from each lane, digested *in situ* with trypsin and analysed by LC-MSMS. Peptides identified in eluates from PL beads were subtracted from peptides identified in eluates from MAA-PL beads. The table indicates the number of unique peptides identified exclusively in eluates from MAA-PL beads. (B+C) Immunoblot for CFH using eluates from either polylysine (PL) or MAA-polylysine (MAA-PL) beads incubated with LDLR<sup>-/-</sup>/RAG<sup>-/-</sup> mouse plasma (B) or human plasma (C). Eluates were separated by SDS-PAGE and blots were probed with CFH-specific antibodies (CFH = 150kD).

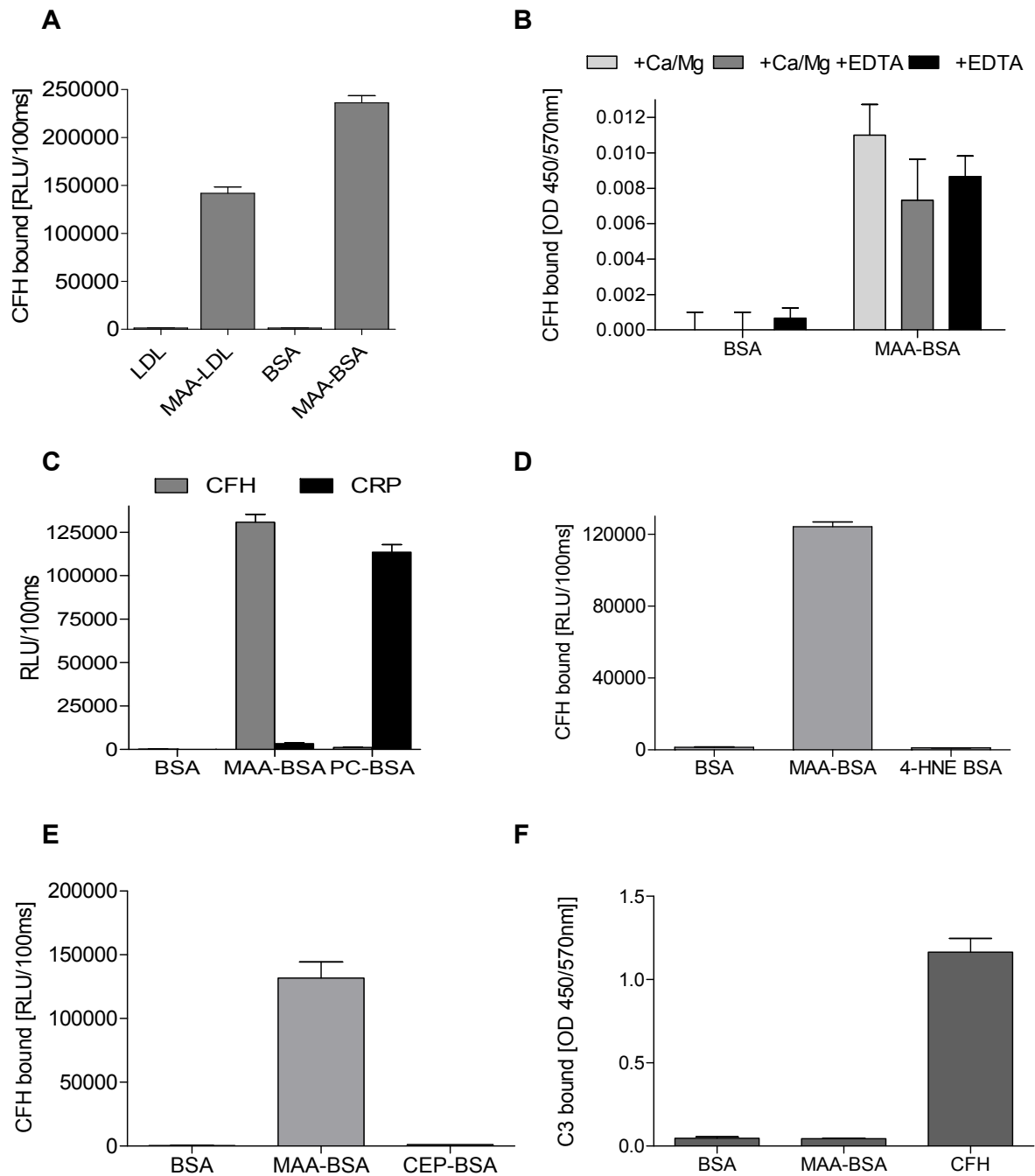


**Fig. 5: CFH interacts directly with MDA-modifications**

(A) ELISA for CFH binding. Shown is the binding of purified CFH (5 $\mu$ g/ml) to coated native LDL, MAA-LDL, BSA and MAA-BSA as determined by chemiluminescent ELISA. Values are given as relative light units (RLU) per 100ms and represent the mean $\pm$ SD of triplicate determinations. This experiment was repeated three times with similar results. (B) ELISA showing the binding of the CFH to coated BSA and MAA-BSA in the presence of MgCl<sub>2</sub> (1mM), CaCl<sub>2</sub> (2mM) and disodium EDTA (10mM). CFH binding was not affected by the addition of the divalent cation-chelator EDTA. Values are given as OD (450/540nm) and represent the mean $\pm$ SD of triplicate determinations. (C) ELISA for CFH and CRP binding. Shown is the binding of purified CFH or CRP (5 $\mu$ g/ml) to coated BSA, MAA-BSA and PC-BSA as determined by chemiluminescent ELISA. Values are given as relative light units (RLU) per 100ms and represent the mean $\pm$ SD of triplicate determinations. (D+E) ELISA for CFH binding. Shown is the binding of purified CFH (2 $\mu$ g/ml) to coated BSA, MAA-BSA and 4-

HNE-BSA (**D**) or CEP-BSA (**E**) as determined by chemiluminescent ELISA. Values are given as relative light units (RLU) per 100ms and represent the mean $\pm$ SD of triplicate determinations. (**F**) ELISA for C3 binding. Shown is the binding of purified C3 (5 $\mu$ g/ml) to coated BSA, MAA-BSA and CFH (a known interactor of C3) as determined by chemiluminescent ELISA. Values are given as relative light units (RLU) per 100ms and represent the mean $\pm$ SD of triplicate determinations.

### 5.3 CFH interacts specifically with MDA-modifications

To characterize the specificity of the binding of CFH to MDA, I performed competition assays. Only MDA- and MAA-modified LDL competed in a concentration dependent manner for the binding of CFH to coated MAA-BSA. Neither native LDL nor the negatively charged Cu<sup>2+</sup>-oxidized LDL used as controls showed any inhibition, thereby excluding non-specific interactions mediated by charge effects (Fig. 6A). To demonstrate a dose-dependent interaction in whole plasma, the binding of CFH to coated MAA-BSA was tested in different plasma dilutions (Fig. 6B). Consistent with the notion that CFH is a major MDA-binding protein in plasma, binding of CFH to coated MAA-BSA was competed by soluble MAA-BSA with similar efficiency in whole plasma (Fig. 6C). Similarly, in a reciprocal experiment, binding of biotinylated MDA-LDL to immobilized purified CFH was fully competed by either MDA- or MAA-modified LDL, even at very low competitor concentrations. Again, neither native LDL nor Cu<sup>2+</sup>-oxidized LDL competed for this binding (Fig. 6D). As an estimate for the affinity, the dissociation constants  $K_d$ s were calculated as 6.4 $\times 10^{-8}$  mol/l for the binding of CFH to coated MAA-BSA and 1.6 $\times 10^{-9}$  mol/l for the binding of MAA-BSA to coated CFH. In the same assay, the monoclonal antibody MDA2, which specifically recognizes MDA-lysine modifications fully inhibited binding of MDA-LDL to CFH. In contrast, the apoB-100 specific monoclonal antibodies MB47 and MB24, which bind to the apoB moiety of MDA-LDL did not inhibit this interaction (Fig. 6E-F). Using plasmon resonance, I observed a concentration dependent binding of CFH to coated MAA-BSA (Fig. 7). Taken together, these findings prove that CFH binds specifically to MDA modifications.

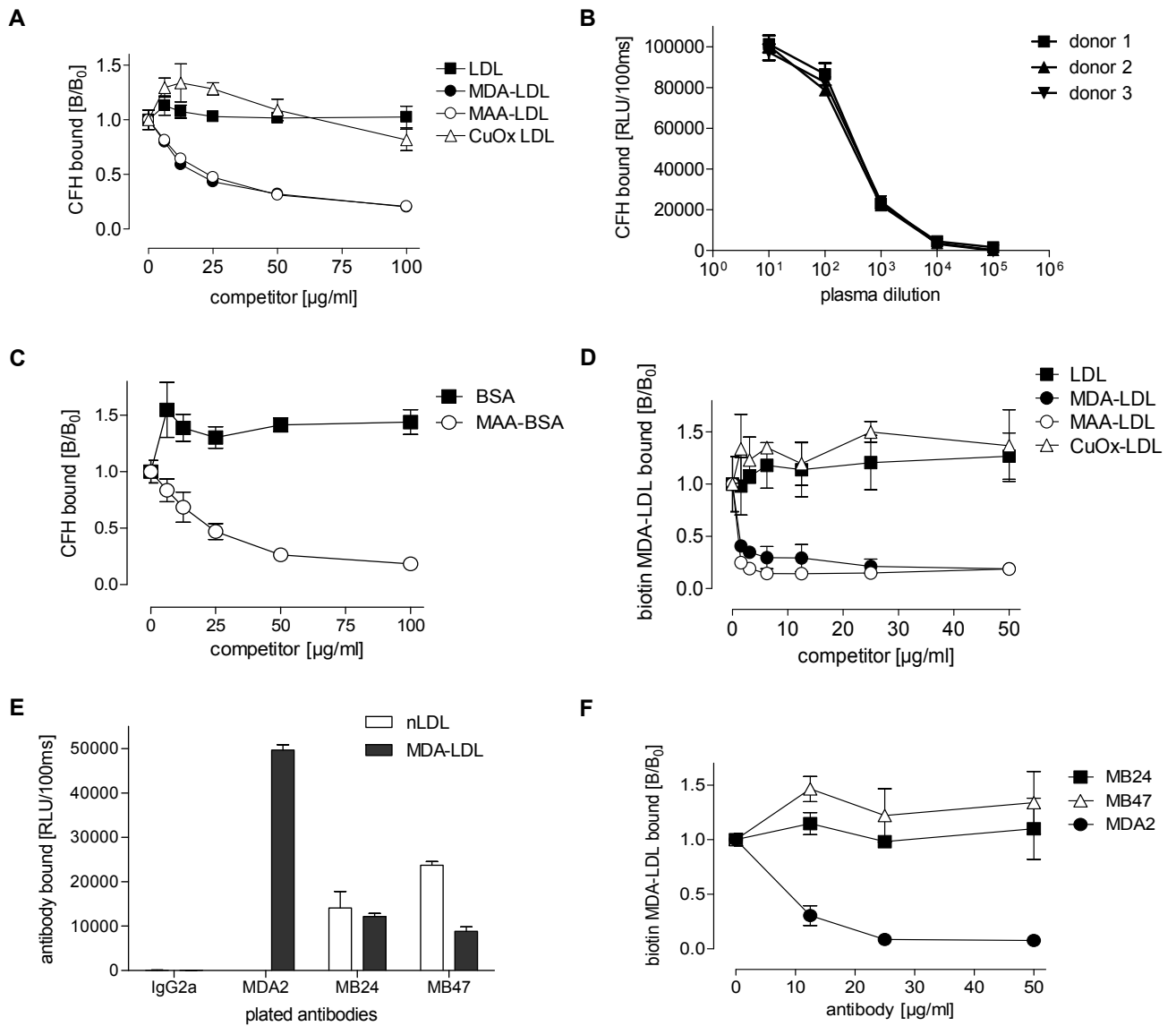


**Fig. 6: CFH binds specifically to MDA-modifications**

(A) Competition immunoassay. The binding of purified CFH to coated MAA-BSA was assessed in the presence of increasing concentrations of LDL, MDA-LDL, MAA-LDL, and CuOx-LDL, or BSA and MAA-BSA. (B) ELISA showing the binding of CFH to coated MAA-BSA in different dilutions of plasma donated by three healthy individuals. Values are given as RLU per 100ms and represent the mean±SD of triplicate determinations. (C) The binding of plasma CFH to coated MAA-BSA was assessed in the presence of increasing concentrations of LDL, MDA-LDL, MAA-LDL, and CuOx-LDL, or BSA and MAA-BSA. (D) Binding of biotinylated MDA-LDL to coated CFH in the presence of increasing concentrations of LDL, MDA-LDL, MAA-LDL and CuOx-LDL. (E) Chemiluminescent immunoassay showing the binding of the MDA2-, MB24-, and MB47 mAbs and an IgG2a isotype control mAb to coated native LDL and MDA-LDL. Bound antibody was detected with AP-conjugated anti-mouse-IgG. Data are the mean of triplicate determinations. (F) Binding of biotinylated MDA-LDL to coated CFH in the presence of increasing concentrations of the ApoB100-specific monoclonal antibodies (mAb) MB24 and MB47 and the MDA-specific mAb MDA2. Data are expressed as a ratio of binding in the presence of competitor (B) divided by the binding in the absence of competitor (B<sub>0</sub>) and represent the mean±SD of triplicate determinations. Shown data are representative of three independent experiments.

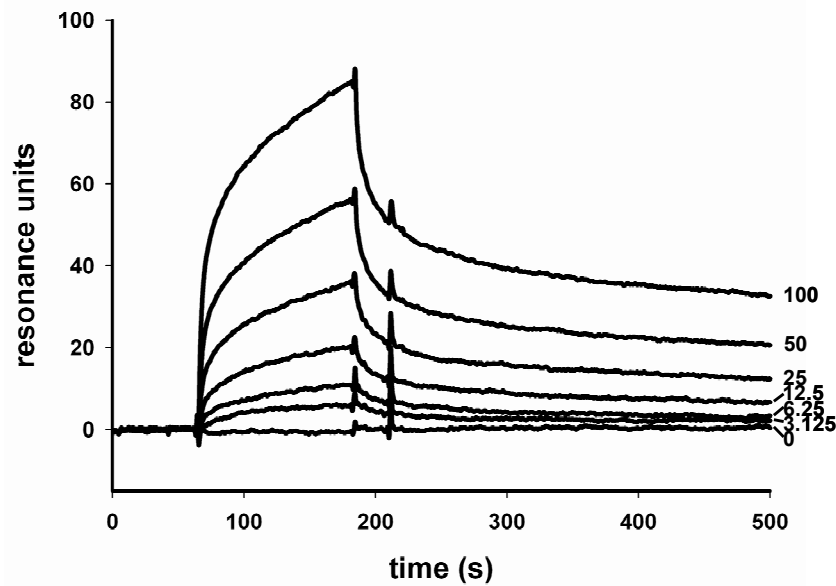


**Fig. 7: Dose dependent interaction of purified CFH with immobilized MAA-BSA**

MAA-BSA was coupled to the flow cell of a CM5 sensor chip. Purified CFH was applied in fluid phase with the indicated concentrations.

#### **5.4 CFH interacts with MDA via SCR 7 and SCR20**

To map the binding site for MDA on CFH, I first tested the binding of CFH in the presence of the monoclonal antibody C18, which binds to the C-terminus of CFH. Preincubation of CFH with C18 abolished its binding to coated MAA-BSA, indicating the involvement of the C-terminal region in this interaction (Fig. 8A). It has been suggested that CFH has a compact form in fluid phase, with the N-terminus binding to the C-terminus, leading to an  $\Omega$ -type structure<sup>54</sup>. Thus, distant domains may come into close proximity and cooperate during ligand binding. To test this possibility, I performed binding studies using recombinantly expressed CFH fragments (Fig. 8B). CFH is composed of 20 closely related globular short consensus repeats (SCRs)<sup>62</sup>. In addition to full length CFH, only fragments containing either SCR7 or SCR20 bound to coated MDA, indicating that either SCR7 or the C-terminal SCR20 was required for the ability of CFH to bind MDA (Fig. 8B). Consistent with this, I could demonstrate in a reciprocal experiment that soluble MDA-LDL only bound to immobilized fragments containing either SCR7 or SCR20, respectively (data not shown). Importantly, these domains have also been identified as clustering points of various disease related mutations<sup>62</sup>.

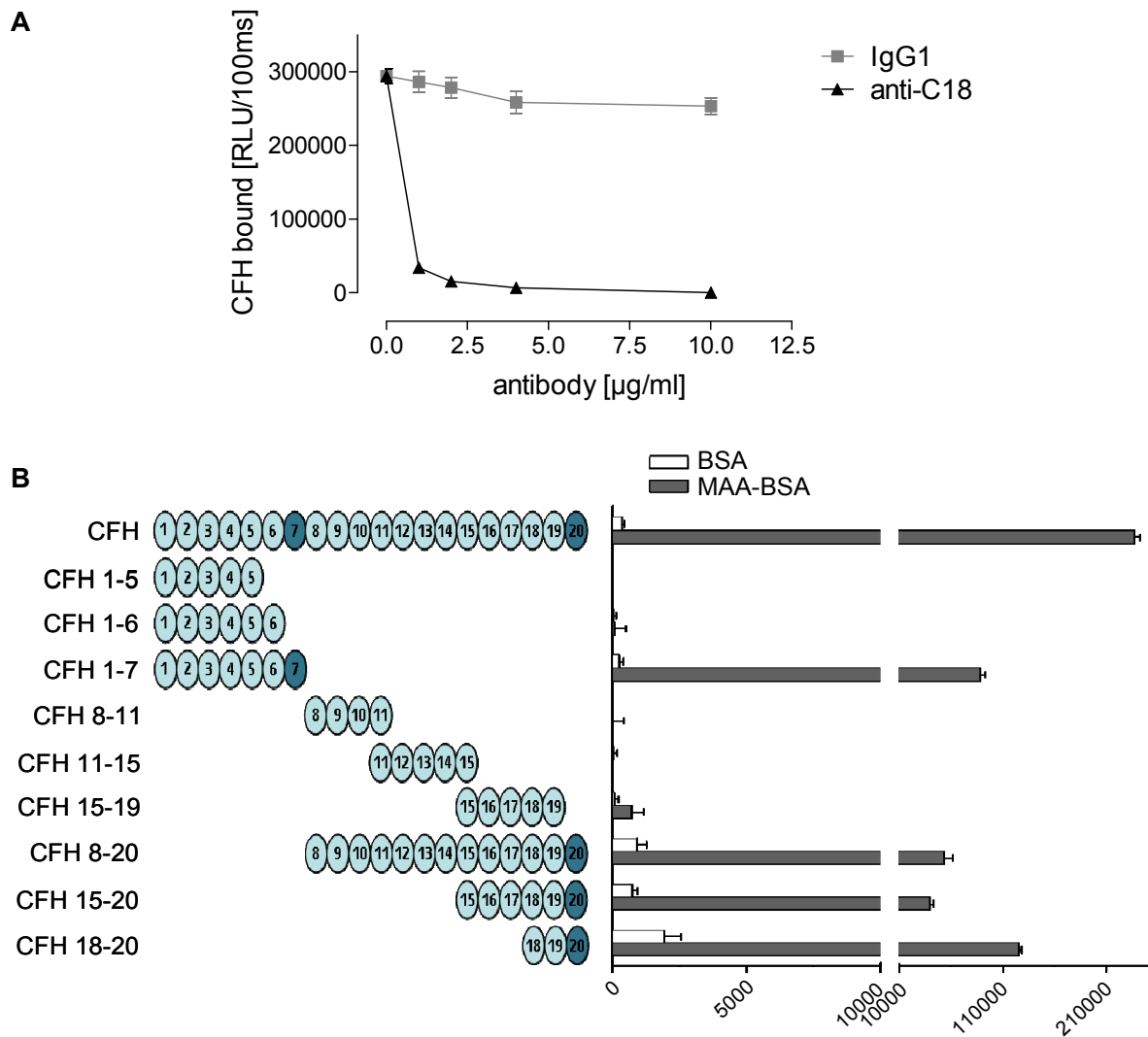


**Fig. 8: The SCR7 and SCR20 domains of CFH are critical for MDA-binding**

(A) CFH was incubated with coated MAA-BSA in the presence of the indicated concentrations of either anti-C18 antibody or isotype matched control antibody. The amount of bound CFH was determined with goat anti-human-CFH antiserum. Each point is the mean of triplicate determinations, expressed as a ratio of CFH binding to MAA-BSA in the presence of competitor to the binding in the absence of competitor ( $B/B_0$ ). (B) ELISA for binding of CFH fragments. The length of CFH fragments used is indicated by schematic representation with each circle depicting one short consensus repeat. Shown is the binding of recombinantly expressed CFH fragments ( $5\mu\text{g/ml}$ ) to coated BSA (white bars) or MAA-BSA (black bars) as determined by chemiluminescent ELISA. Values are given as RLU per 100ms and represent the mean $\pm$ SD of triplicate determinations.

## 5.5 The AMD-associated CFH SNP rs1061170 leads to impaired binding to MDA

One of the most widely studied single nucleotide polymorphism (SNP) in *CFH* is the prevalent rs1061170 SNP, which causes an amino acid switch on position 402 (Y→H) in SCR7. Because I found that SCR7 is important for the interaction with MDA, I tested the effect of the H402 substitution. I purified CFH from the plasma of homozygous individuals expressing either CFH Y402 or CFH H402, respectively, and tested the binding to MDA. Compared to CFH of the common Y402 variant, the CFH variant H402 exhibited significantly impaired binding to plated MAA-BSA (Fig. 9A). The H402 variant has been associated with a significant risk for the development of AMD<sup>37-40</sup>. Therefore, I analyzed the binding of CFH to coated MDA-LDL in plasma samples of AMD-patients with the respective genotypes. Compared to the extent of CFH binding to MDA-LDL using plasma of individuals homozygous for the protective allele, binding was reduced by 23% ( $p < 0.001$ ) in plasma of heterozygous subjects, and by 52% ( $p < 0.001$ ) in plasma of subjects homozygous for the H402 risk allele (Fig. 9B), irrespective of the total plasma CFH levels (Fig. 9C). Moreover, plasma levels of MDA specific IgM and IgG antibodies were similar in the different groups (Fig. 9D-E). Using an additive model, I calculated the association of rs1061170 with CFH-binding to MDA with  $p = 1.29^{-40}$ . Similar results have been found in five separate experiments using other MDA-type antigens and a wide variety of plasma dilutions (data not shown). These data are consistent with the results obtained with the purified CFH variants described above. The genetic deletion of CFH related proteins 1 and 3 has been reported to protect from AMD development and could influence CFH binding to MDA<sup>79</sup>. Less than 25% of the cohort used in this study carried deletions at these loci and removal of these individuals from the analysis did not alter the significance of the association of rs1061170 with MDA-binding (Fig. 9F). The significantly impaired ability of the risk variant to bind MDA suggested an important role for this interaction in AMD pathogenesis.

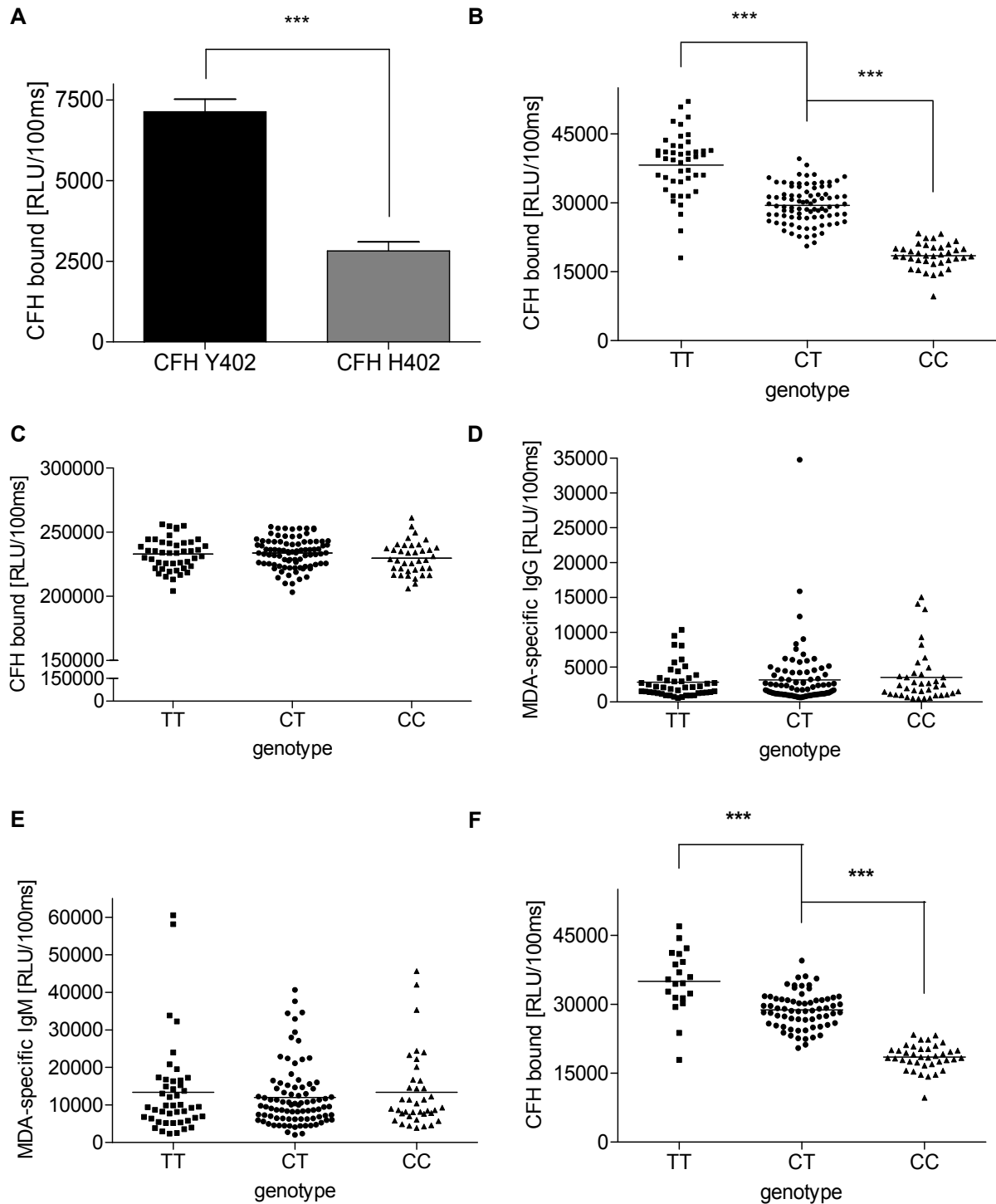


**Fig. 9: The AMD associated H402 variant displays strongly impaired MDA-binding**

(A) ELISA for binding of CFH variants. Shown is the binding of purified CFH variant Y402 and CFH variant H402 (both at  $1\mu\text{g/ml}$ ) to coated MAA-BSA as determined by chemiluminescent ELISA. CFH H402 showed significantly lower binding to MAA-BSA compared to CFH Y402. Values are given as RLU per 100ms and represent the mean $\pm$ SD of triplicate determinations. This experiment was repeated three times with similar results. (B) ELISA for binding of plasma CFH in subject plasma according to genotype. Plasma of subjects homozygous for the H402 allele (CC, n=38), heterozygous for the H402 allele (CT, n=88) or homozygous for the wildtype Y402 allele (TT, n=45) was diluted

1:250 and added to microtiter wells coated with MDA-LDL. The relative amount of CFH binding was then determined by chemiluminescent ELISA using a biotinylated guinea pig anti-mouse-CFH antibody. There was a significant gene-dosage dependent reduction in binding of CFH to MDA-LDL related to the H402 (C) allele. Symbols represent individual subject samples with horizontal bars indicating the mean of each group. Values are given as RLU per 100ms and represent the mean±SD of triplicate determinations (\*\*\*)  $p < 0.001$ . (C) ELISA showing the total amount of CFH in subject plasma according to genotype. Plasma of subjects was diluted 1:250 and added to microtiter wells coated with guinea pig anti-CFH. The relative amount of CFH binding was then determined by chemiluminescent ELISA using the biotinylated guinea pig anti-mouse-CFH antibody. Symbols represent individual subject samples with horizontal bars indicating the mean of each group. Values are given as RLU per 100ms and represent the mean of triplicate determinations. (D+E) ELISA for binding of IgG (D) and IgM (E) in subject plasma according to genotype. Plasma was diluted 1:250 and added to microtiter wells coated with MDA-LDL. The relative amount of IgG or IgM binding was then determined by chemiluminescent ELISA using secondary anti-IgG or anti-IgM antibodies. There was no association with the binding of IgG or IgM to MDA-LDL related to the H402 (C) allele. Symbols represent individual subject samples with horizontal bars indicating the mean of each group. Values are given as RLU per 100ms and represent the mean of triplicate determinations. (F) ELISA for binding of plasma CFH in subject plasma according to genotype. Subjects carrying CFHR1 or CFHR3 deletions were excluded. Plasma of subjects homozygous for the H402 allele (CC, n=38), heterozygous for the H402 allele (CT, n=67) or homozygous for the wildtype Y402 allele (TT, n=20) was diluted 1:250 and added to microtiter wells coated with MDA-LDL. The relative amount of CFH binding was then determined by chemiluminescent ELISA using the biotinylated guinea pig anti-mouse-CFH antibody. A significant gene-dosage dependent reduction in binding of CFH to MDA-LDL related to the H402 (C) allele could be observed. Symbols represent individual subject samples with horizontal bars indicating the mean of each group. Values are given as RLU per 100ms and represent the mean of triplicate determinations. (\*\*\*)  $p < 0.001$ .

## 5.6 CFH binds cellular debris via MDA-epitopes

Due to constant light exposure, the retina provides a highly oxidative environment that facilitates lipid peroxidation<sup>80</sup>. I detected MDA-epitopes in histological sections of two patients without AMD and five with AMD using a specific antibody. MDA-epitopes were detectable throughout the choroid and Bruch's membrane (Fig. 10A, D). In eyes without AMD, labeling for MDA was stronger in the outer than inner Bruch's membrane (Fig. 10A). In eyes with AMD, MDA staining was seen diffusely throughout Bruch's membrane (Fig. 10D). Staining for CFH followed a similar topographical pattern (Fig. 10B, E). In addition, strong CFH labeling was seen in the RPE and choriocapillaris basement membranes. Moreover, the presence of C3d, a cleavage product of iC3b, was documented, indicating co-factor activity at the same sites (Fig. 10C, F). Respective isotype control antibodies did not show positive staining (Fig. 10G, H, I). I further demonstrated by confocal microscopy the presence of MDA-epitopes on the surface of *in vitro* generated necrotic retinal pigment epithelial cells, which is a major cell type affected in AMD. Moreover, I could show that

CFH bound to these necrotic cells co-localized with the presence of MDA-epitopes, suggesting that MDA mediates the recognition of dying cells by CFH (Fig. 10J).

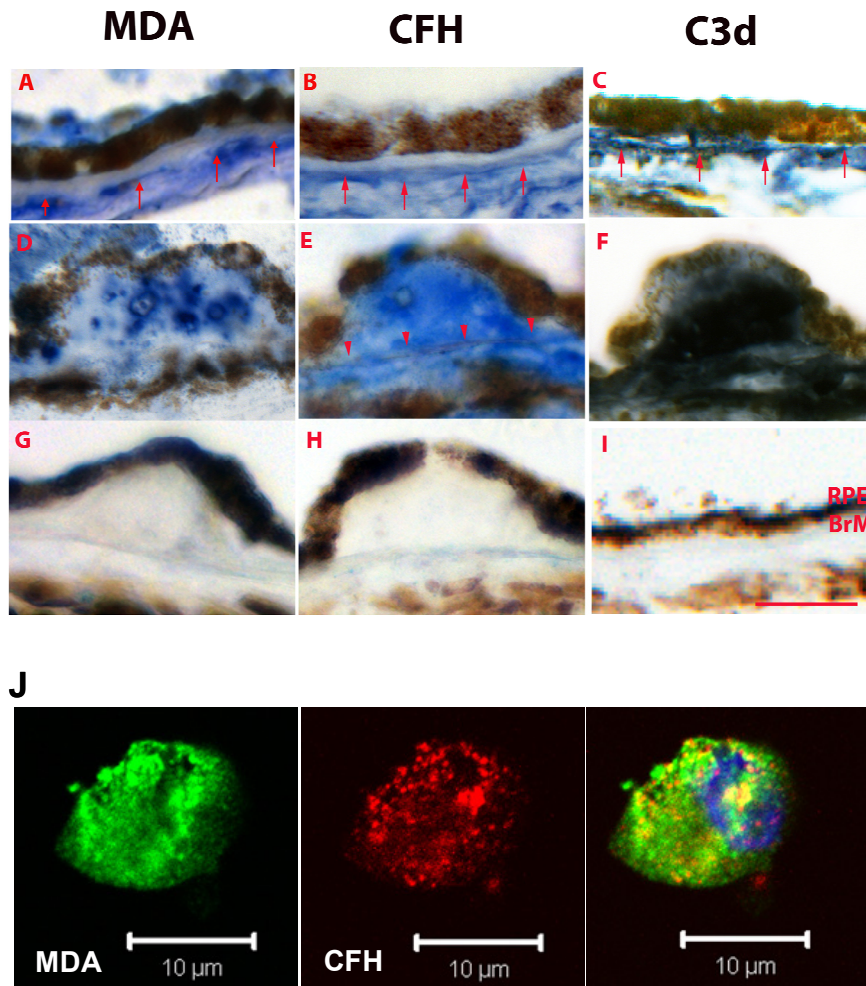


**Fig. 10: CFH binds to MDA-epitopes present in AMD lesions and on necrotic cells**

(A-I) Immunohistochemistry of MDA (left), CFH (middle), and C3d (right) localization in human maculas. For a 72 year old subject heterozygous for the Y402H SNP without AMD, strong labeling (red arrows) for MDA (A), CFH (B), and C3d (C) is seen in outer relative to inner Bruch's membrane (BrM). For a 93 year old subject homozygous for the Y402H SNP with AMD, diffuse staining is seen in Bruch's membrane. Additional staining for MDA (D), CFH (E), and C3d (F) is seen in a drusen deposit. Strong labeling for CFH is seen in the RPE basement membrane (red arrowheads). Respective IgG control immunostains are shown in (G), (H), and (I). Bar=25µm. Sections are representative for 7 donors (5 AMD, 2 controls). (J) Confocal immunofluorescent photograph of necrotic retinal pigment epithelium cells stained with the MDA-specific murine IgM NAb EO14 (left panel, green) and a CFH-specific antibody (middle panel, red), respectively. The right panel shows a merged picture indicating colocalization of CFH binding with the presence of MDA-epitopes (yellow).

To demonstrate this directly, I used flow cytometry to assess the binding of CFH to apoptotic blebs from Jurkat T-cells in the presence of MAA-BSA as competitor. Consistent with the fact that MDA-epitopes are present only on a subgroup of apoptotic blebs, I found that CFH bound between 5 to 45% of apoptotic blebs (Fig. 11A). Importantly, MAA-BSA competed for this binding by more than 60%, while unmodified BSA did not have an effect (Fig. 11B). These data demonstrate that MDA-adducts present in several retinal compartments and on the surface of necrotic retinal pigment epithelial cells represent *in vivo* ligands for CFH.

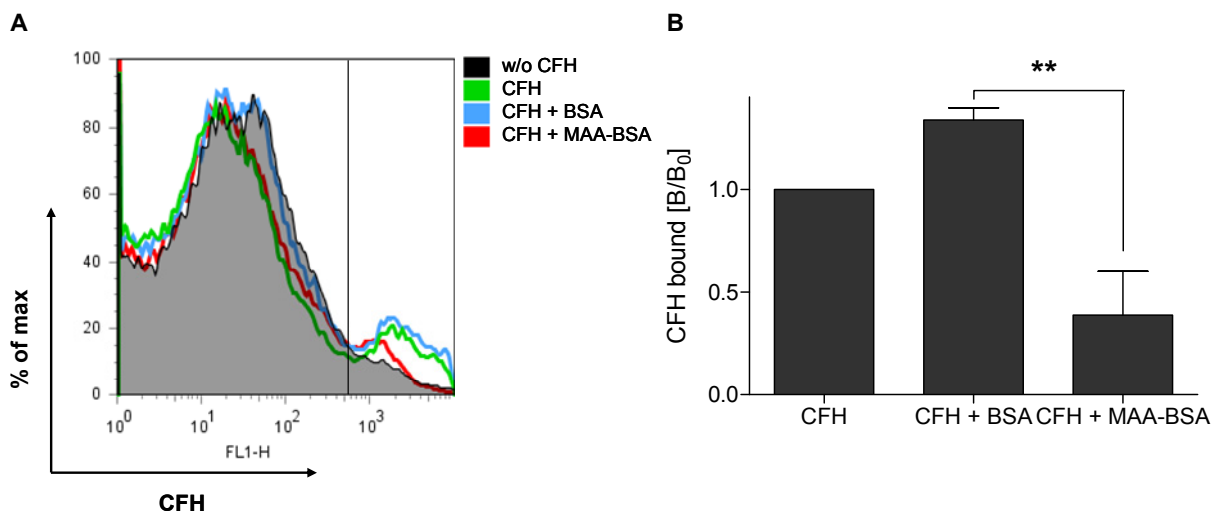


**Fig. 11: MAA-BSA competes for the binding of CFH to apoptotic blebs**

Competition assay for the binding of CFH to apoptotic blebs. **(A)** Shown is a representative FACS histogram showing CFH binding to apoptotic blebs in the absence and presence of BSA and MAA-BSA, respectively. CFH-binding is indicated by FITC-fluorescence on the abscissa. **(B)** Binding of CFH to apoptotic blebs from Jurkat T-cells was assessed either alone or in the presence of BSA or MAA-BSA by flow cytometry. In the presence MAA-BSA, binding of CFH to apoptotic blebs was significantly inhibited. Shown is the ratio of CFH binding in the presence of competitor (B) divided by the binding in the absence of competitor ( $B_0$ ) based on mean fluorescence intensity. Data represent the mean $\pm$ SEM of four independent experiments (\*\*  $p < 0.01$ ).

## 5.7 CFH inactivates complement on MDA-bearing surfaces

An important complement regulatory activity of CFH lies within its capacity to act as a co-factor for the serine protease factor I, thereby promoting the degradation of C3b into inactive iC3b fragments. This is also important, as the deposition of iC3b on apoptotic cells increases their clearance in an anti-inflammatory manner<sup>81, 82</sup>. I therefore tested whether CFH induces iC3b generation when bound to immobilized MDA. Indeed, CFH resulted in the formation of iC3b in a dose- and time-dependent manner when bound to coated MAA-BSA (Fig. 12A-B). When comparing the co-factor activity of the 402 variants on MDA-decorated surfaces, I discovered a strong functional difference in that impaired MDA-binding of the risk variant led to severely reduced factor I mediated C3 cleavage (Fig. 12C-D). This activity of CFH may represent an important protective mechanism in conditions in which MDA is continuously generated, e.g. on the surface of dying cells.

Importantly, other members of the CFH family such as CFHR1 and CFHR3 share high sequence homology with the C-terminus of CFH and therefore contain a potential MDA-binding site without possessing co-factor activity for factor I. Indeed, in an immunoassay, purified CFHR1 binds to MDA. Using a recombinant construct comprising only the C-terminal domains of CFHR1, I could confirm that this interaction is mediated via the C-terminal domains (Fig. 12E). Deletions of CFHR1/3 have been reported to be protective in AMD<sup>79</sup>, suggesting a negative role of these proteins in this pathology. To demonstrate the potential capacity of MDA-binding CFHR to inhibit the beneficial co-factor activity of CFH, I tested the ability of C-terminal CFH fragments to compete for the co-factor activity by binding to MDA. Indeed, the MDA-binding fragment SCR18-20 prevented full length CFH from inducing iC3b generation, whereas a non-binding fragment containing SCR15-19 had no effect (Fig. 12F). These data point towards a complex regulation of complement activation on MDA-decorated surfaces that involves other members of the CFH protein family.

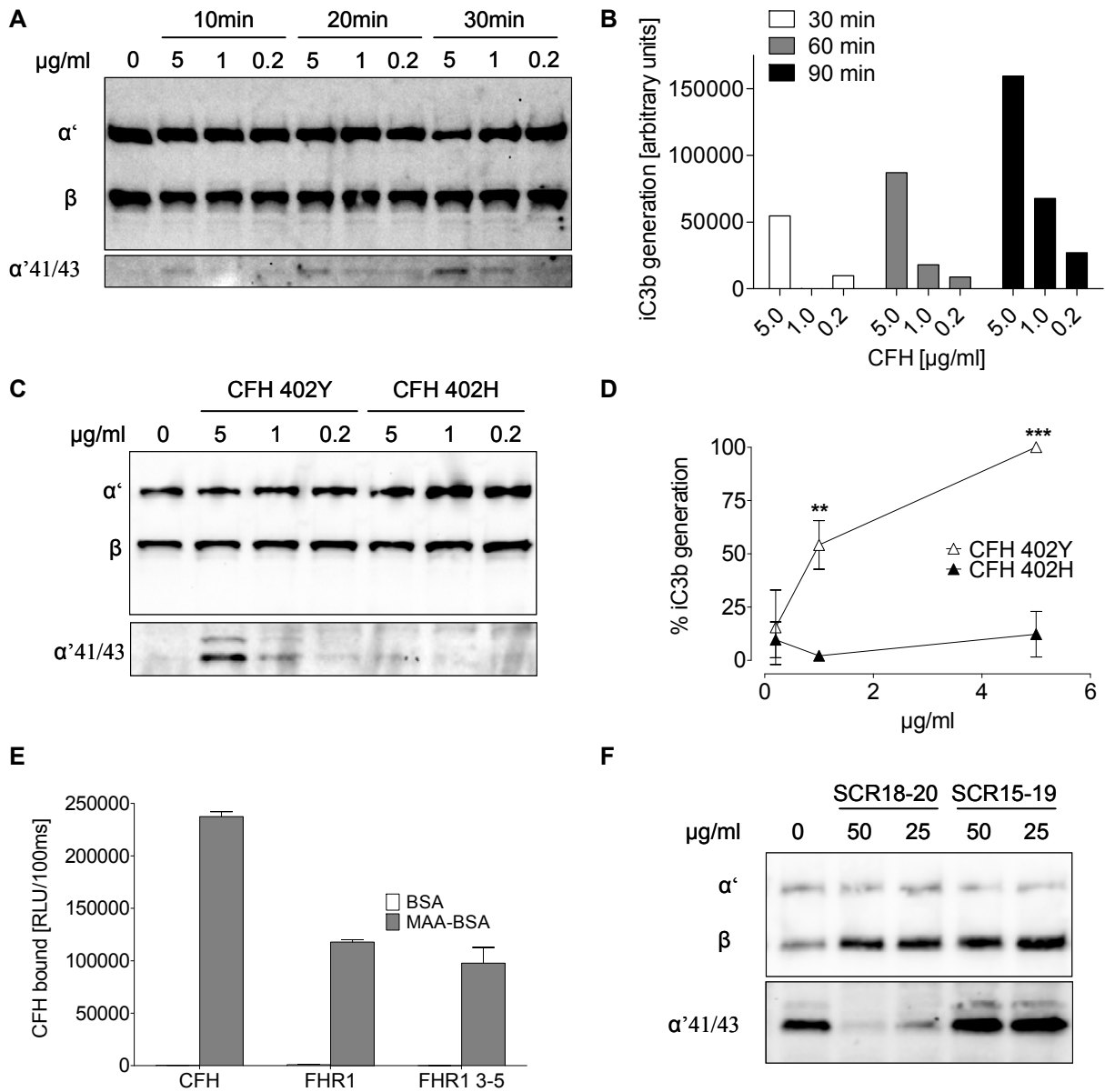


**Fig. 12: CFH inhibits complement activation on MDA-decorated surfaces**

(A+B) CFH bound to coated MAA-BSA was incubated with C3b and factor I for the indicated times and the generation of C3b degradation products was visualized by immunoblotting (A). The 43kDa degradation product iC3b was densitometrically quantified. The results are presented as a bar graph (B). (C+D) CFH variants bound to coated MAA-BSA were incubated with C3b and factor I and the generation of C3b degradation products was visualized by immunoblotting. α'41/43 indicates iC3b products that are cleaved off the alpha chain of C3b. β indicates the beta chain of C3b, that remains uncleaved and served as a loading control. Shown is a representative blot of four independent experiments (C). The 41/43kDa degradation product C3b was densitometrically quantified and the activity of the protective CFH Y402 variant was set to 100%. Shown is the mean±SEM of three independent experiments (D). (E) Chemiluminescent immunoassay showing the binding of CFH, CFHR1 and recombinantly expressed CFHR1 SCR3-5 to coated BSA and MAA-BSA. Based on this, CFHR1 interacts with coated MAA-BSA via SCR3-5. Data are the mean of triplicate determinations. (F) CFH was added to coated MAA-BSA in the presence of either CFH 18-20 or CFH 15-19 and subsequently incubated with C3b and factor I. The generation of C3b degradation products was visualized by immunoblotting. Shown is a representative blot of two independent experiments.

## 5.8 CFH inhibits MDA-induced responses in vitro

The inflammatory process in AMD lesions has been suggested to be propagated by the secretion of cytokines including IL-8 and the recruitment of macrophages<sup>83,35</sup>. Therefore, I first tested the effect of MDA on retinal pigment epithelial cells, the main cell type involved in AMD. Stimulation with MAA-BSA induced the expression of IL-8 in ARPE-19 cells (Fig. 13A). Moreover, it caused an antioxidant response as indicated by the upregulation of NAD(P)H dehydrogenase and hemoxygenase-1 (Fig. 13A). I then tested the effect of CFH on the binding and uptake of MAA-LDL by macrophages. In a cell-based ELISA, CFH almost completely inhibited the binding of MAA-LDL to thioglycollate-elicited macrophages in a dose-dependent manner (Fig. 13B). This indicates that CFH binds to the same epitope on MAA-LDL that is necessary for its recognition by macrophages. In line with this, CFH blocked the uptake of MDA-LDL in thioglycollate-elicited macrophages by 70% (Fig. 13C). Subsequently, I tested the capacity of MDA to induce the expression of inflammatory genes in monocytic THP-1 cells. Similar to ARPE-19 cells, THP-1 cells exhibited a robust expression of IL-8 following MAA-BSA stimulation. In addition, MAA-BSA induced the expression of TNF $\alpha$  and IL-1 $\beta$ , but not of IL-12 $\beta$  (Fig. 14). I then tested the ability of CFH to neutralize this pro-inflammatory process. MAA-BSA strongly stimulated the secretion of IL-8, which was inhibited by physiological concentrations of CFH in a dose dependent manner (Fig. 15A). In contrast, CFH had no effect on IL-8 production induced by phorbol myristate acetate (Fig. 15B).

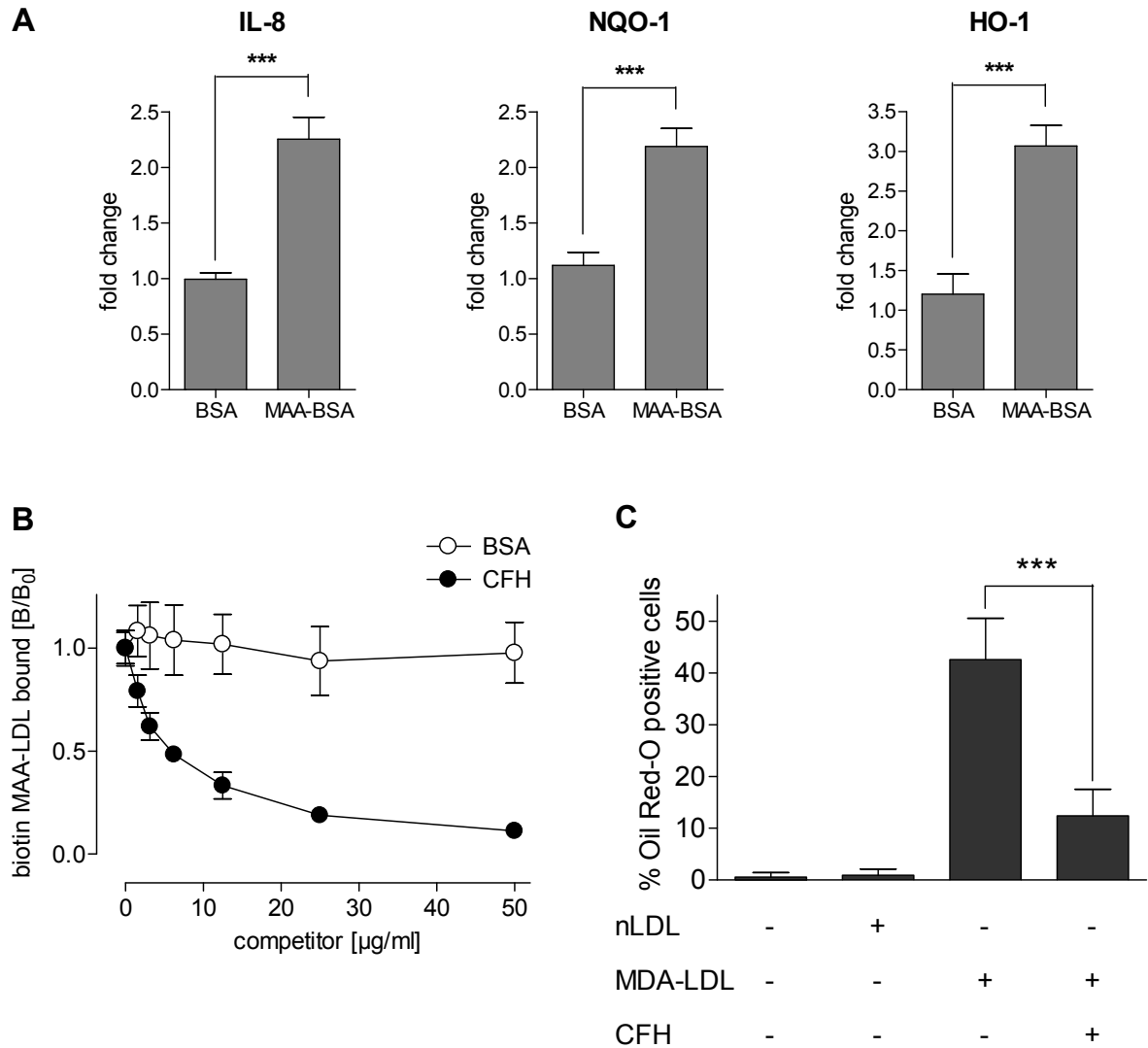


**Fig. 13: CFH inhibits binding and uptake of MDA in vitro**

(A) Relative mRNA expression levels of indicated genes obtained by real-time RT-PCR. ARPE-19 cells were cultured with 50 $\mu\text{g/ml}$  BSA or MAA-BSA for 24h before RNA extraction. Expression was normalized to BSA-treated control. Data represent the mean $\pm$ SEM of three independent experiments. (B) Binding of biotinylated MAA-LDL to thioglycollate elicited macrophages was assessed in the presence of increasing concentrations of BSA (open circles) or CFH (filled circles) using a cell based chemiluminescent ELISA. Data are expressed as a ratio of binding in the presence of competitor (B) divided by the binding in the absence of competitor ( $B_0$ ) and represent the mean $\pm$ SD of triplicate determinations. The experiment was repeated 3 times with similar results. (C) Thioglycollate elicited macrophages were incubated with native LDL or MDA-LDL (all at 50 $\mu\text{g/ml}$ ) in the absence or presence of CFH (200 $\mu\text{g/ml}$ ) for 24h. After fixation, cells were stained for neutral lipids using Oil Red-O and the number of Oil Red-O positive cells was quantified among at least 500 cells counted. The bars indicate mean $\pm$ SD percentage of Oil Red-O positive cells of triplicate determinations from two independent experiments (\*\*\*)  $p < 0.001$ .

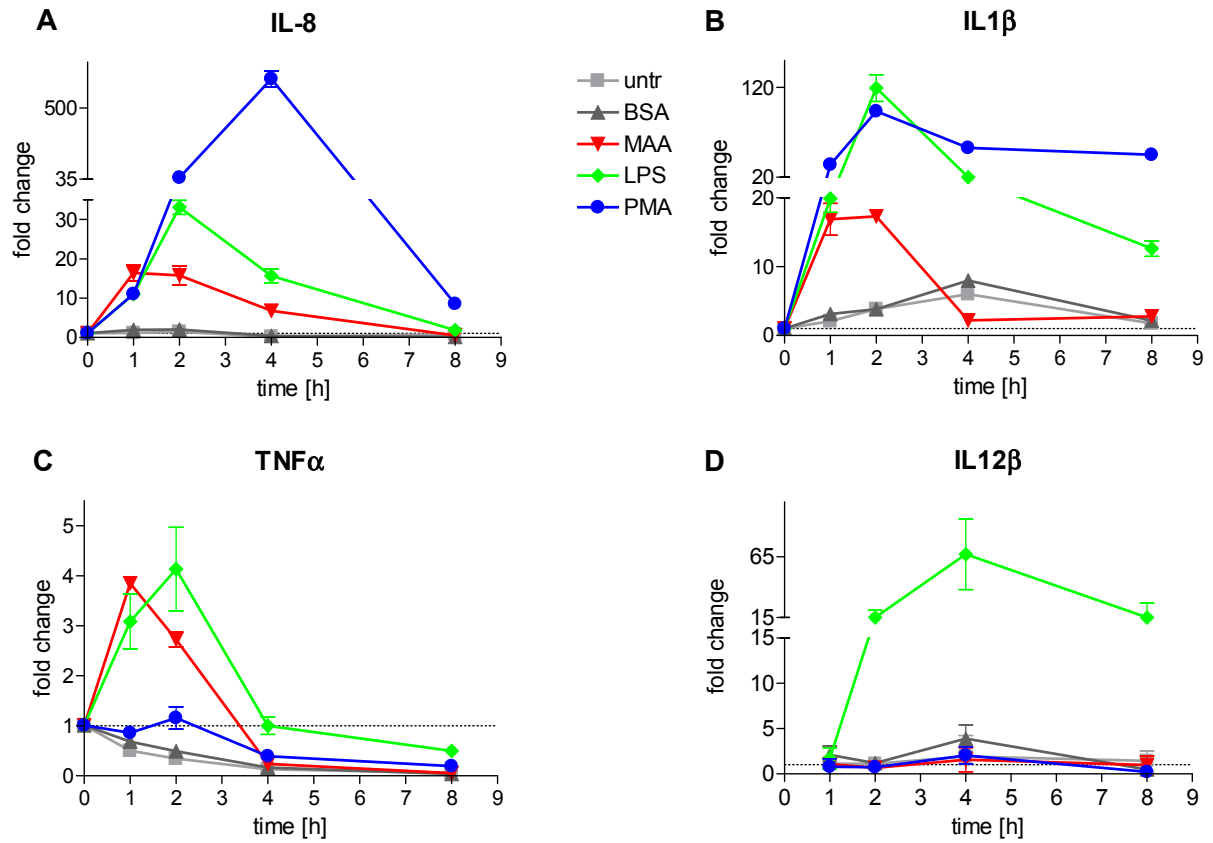


**Fig. 14: MAA-BSA induces an immediate inflammatory response in THP1 cells**

THP1 cells were stimulated with BSA, MAA-BSA, LPS or PMA. After the indicated times, expression of IL12β, IL1β, TNFα and IL8 was determined by RT-qPCR. Data points represent mean±SD of biological triplicates.

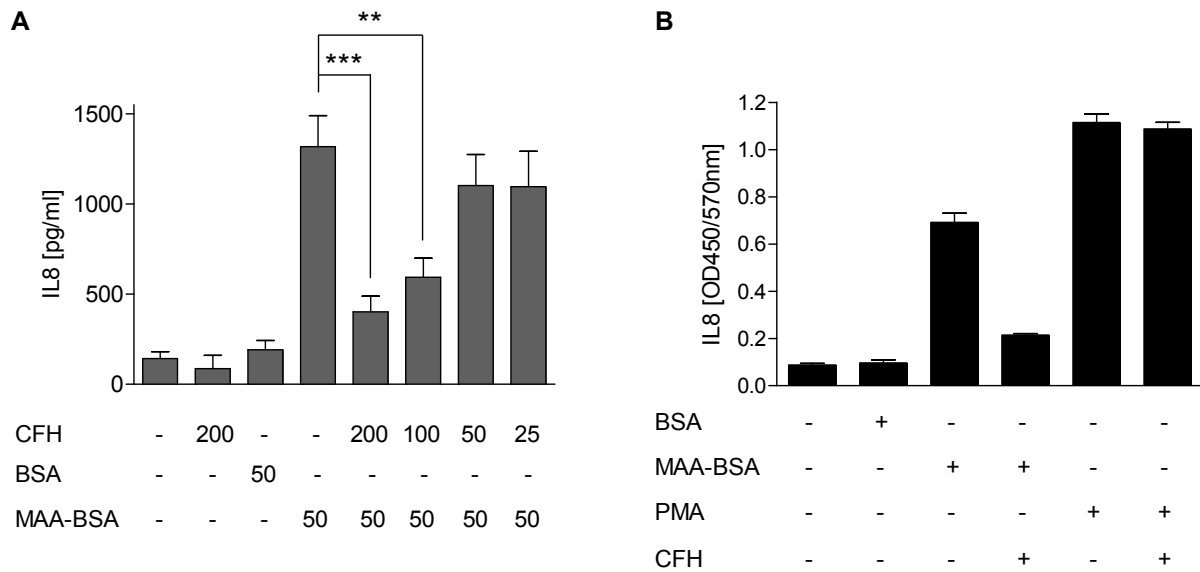


**Fig. 15: CFH inhibits the MDA-response in vitro**

(A) THP-1 cells were cultured under indicated conditions for 12h and supernatants were assayed for the presence of IL-8 by ELISA. Numbers below indicate concentrations of CFH, BSA and MAA-BSA in  $\mu\text{g/ml}$ . Bars represent mean $\pm$ SEM of triplicate determinations from three independent experiments. (B) THP1 cells were cultured in the presence of BSA, MAA-BSA, CFH and/or PMA for 16h and supernatants were assayed for the presence of IL-8 by ELISA. Bars represent mean $\pm$ SD of triplicate determinations.

## 5.9 CFH inhibits MDA-induced responses in vivo

To evaluate the importance of this interaction in vivo, I examined the effect of MAA-BSA in a murine model. I first validated that MAA-BSA could induce the secretion of growth-regulated alpha protein (KC), the mouse orthologue to human IL-8, in murine bone marrow derived as well as peritoneal macrophages. Indeed, MAA-BSA induced a strong expression of KC in both types of primary macrophages (Fig. 16A and data not shown). To test the proinflammatory effect of MAA-BSA as well as the scavenging capacity of CFH in an AMD relevant site, I performed intravitreal microinjections of MAA-BSA with or without CFH. After six hours, mice were sacrificed, RPE/choroid was isolated from the eye after enucleation, and RNA was extracted. The purity of the preparation was confirmed by demonstrating the expression of the RPE-specific gene *RPE65* in all samples and the lack of rhodopsin-expression as a marker for the neurosensory retina (Fig. 16B). MAA-BSA injection led to a 7-fold upregulation of KC expression in these RPE-preparations, while BSA-injection had no effect. Importantly, addition of CFH completely inhibited the effect

induced by MAA-BSA (Fig. 16C). Thus, MAA-adducts promote inflammatory responses in different cell types involved in AMD *in vitro* and in the eye *in vivo*, and CFH specifically neutralizes this property.

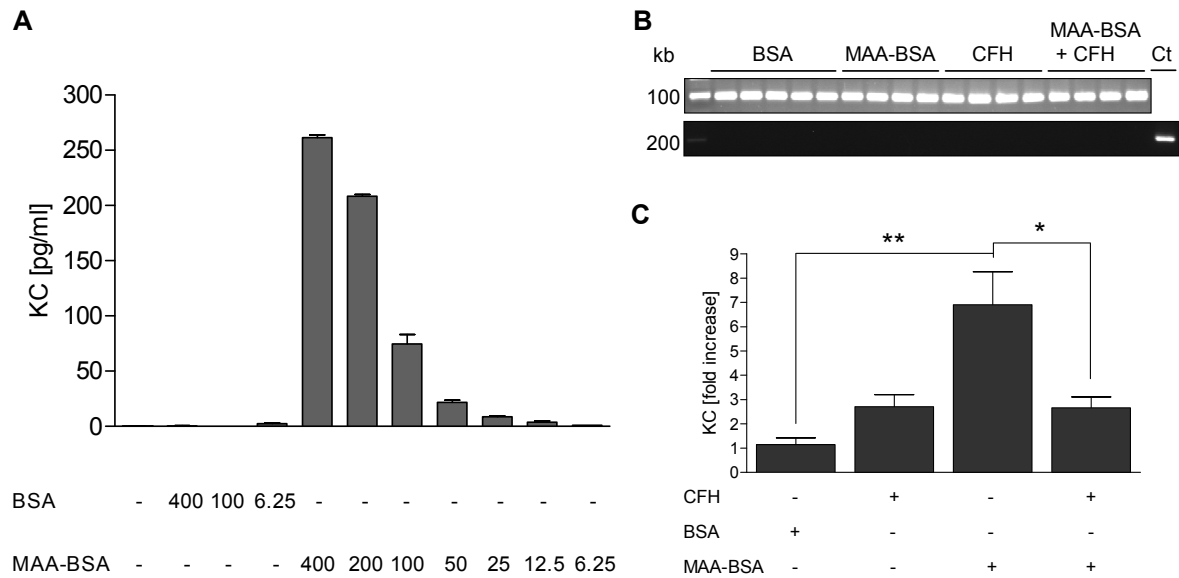


**Fig. 16: CFH inhibits the MDA-response in vivo**

(A) Mouse bone marrow derived macrophages were cultured in the presence of indicated concentrations of BSA or MAA-BSA for 16h and supernatants were assayed for the presence of KC by ELISA. Numbers below indicate concentrations of BSA and MAA-BSA in  $\mu\text{g/ml}$ . Bars represent mean $\pm$ SD of triplicate determinations. (B-C) Mice were injected intravitreally with BSA, MAA-BSA and/or CFH. Six hours after injection, RPE/choroid was isolated. (B) RT-PCR on cDNA generated from RPE/choroid fractions with primers amplifying *RPE65*, an RPE specific gene and *RHO*, a gene expressed in the neurosensory retina only. cDNA isolated from neurosensory retina was used as a control (Ct). (C) Expression of KC was assessed by RT-qPCR. Bars and error bars represent group mean $\pm$ SEM, respectively (\*  $p < 0.05$ , \*\*  $p < 0.01$ , \*\*\*  $p < 0.001$ ).

## 6. DISCUSSION

In this thesis, I report the identification of CFH as a hitherto unrecognized innate defense protein against the lipid peroxidation product MDA. MDA is ubiquitously generated under conditions of oxidative stress and is widely used as a marker thereof. My unbiased approach to identify MDA-binding plasma proteins by mass spectrometry yielded CFH as the most dominant MDA-binding protein in plasma, besides MDA-specific antibodies. I provide several lines of evidence that the interaction between MDA and CFH is of very high specificity and affinity. MDA-adducts are prominently found in inflammatory settings and were shown to initiate and propagate inflammatory processes<sup>1, 23, 84</sup>. Consequently, MDA should represent a critical target for endogenous host defense mechanisms. My thesis laboratory recently showed that a considerable fraction of innate IgM NAb binds to apoptotic cells via MDA epitopes<sup>17</sup>. Moreover, a germline encoded natural IgM antibody with specificity for MDA was identified that had the capacity to promote clearance of apoptotic cells in mice<sup>17</sup>. My discovery of CFH as an MDA-binding protein further supports the notion that innate immunity plays a pivotal role not only in the immediate defense against invading microbes, but also in providing a homeostatic response against endogenous oxidation-specific danger associated molecular patterns<sup>10</sup>. This is consistent with earlier findings showing that another oxidation-specific epitope, the phosphocholine headgroup of oxidized phosphatidylcholine, is a ligand for three different types of innate effector proteins: The macrophage scavenger receptors CD36 and SR-B1<sup>11, 85</sup>, the murine IgM NAb EO6/T15<sup>15, 16</sup> and the acute phase reactant C-reactive protein<sup>14</sup>. In an analogous manner, MDA is recognized by macrophage scavenger receptor SR-A<sup>86</sup>, several germline IgM NAb, and - as I now demonstrate - by CFH. Thus, my new finding supports the general paradigm, in which oxidation specific epitopes are recognized by an array of innate immune receptors.

CFH is one of the most abundant proteins in plasma (~100 to 700 µg/ml)<sup>46</sup> and the major regulator of complement activation<sup>87</sup>. It limits complement amplification through interference at the level of the C3 convertase - an enzymatic protein complex that is essential for the propagation of all complement pathways<sup>87</sup>. This property allows CFH to mediate important housekeeping functions by protecting self cells from complement activation<sup>88</sup>, which is especially important for apoptotic and necrotic cells that lose other surface associated complement regulators<sup>89</sup>. In this regard, the ability of CFH to bind dying cells is

increasingly recognized as an important anti-inflammatory mechanism. CFH ensures that complement activation is limited to the initial steps of C3b opsonization and reduces further inflammatory responses like the generation of C5a<sup>90</sup>. A number of potential ligands for CFH on host cells have been studied, including glycosaminoglycans<sup>55</sup>, as well as Annexin A2, DNA, and histones<sup>91</sup> on the surface of apoptotic cells. In the direct identification of MDA as a major ligand for CFH on apoptotic/necrotic cells, I have identified a molecular mechanism by which CFH prevents excessive complement activation by such endogenous triggers. Indeed, I show that MDA epitopes provide a surface for CFH to allow local generation of anti-inflammatory iC3b fragments. Furthermore, CFH was shown to cooperate with CRP in promoting the uptake of apoptotic cells by THP1 macrophages *in vitro*<sup>92</sup>. CRP is a potent trigger of the classical complement pathway and also binds to apoptotic cells via another oxidation specific epitope, PC of oxidized phospholipids<sup>14</sup>. Therefore, the presence of MDA and PC on apoptotic cells may result in efficient co-recruitment of CFH and CRP, respectively, thereby limiting the CRP induced complement activation and facilitating the uptake. Consequently, impaired binding of CFH to MDA may result directly or indirectly in propagated inflammation. This protective capacity of CFH becomes highly relevant in situations of increased oxidative stress and when large amounts of cellular debris are generated. In addition, accumulating evidence demonstrates that necrotic and, under certain conditions, apoptotic cells are pro-inflammatory *per se*<sup>93, 94</sup>. Hence, the interaction of CFH with MDA-modified cellular compounds is also relevant because the same epitope that is recognized by CFH mediates their recognition by macrophages and has the capacity to induce IL-8 secretion. In fact, this offers an explanation for the recently reported ability of CFH to reduce endothelial IL-8 secretion in response to apoptotic blebs<sup>92</sup>. Thus, CFH possesses an additional housekeeping function by binding MDA and preventing adverse reactions induced by MDA. MDA-epitopes are responsible for the recruitment of CFH to the surface of apoptotic cells, where it neutralizes their pro-inflammatory properties and halts complement activation.

I found that SCR7 and SCR20 mediate the binding of CFH to MDA. These two domains are clustering sites for mutations associated with AMD, but also other diseases such as membranoproliferative glomerulonephritis and atypical hemolytic uremic syndrome<sup>87</sup>. The H402 exchange in SCR7 is the most prominent example: patients with the CC genotype (leading to homozygous H402 substitution) are 6-7 times more likely to develop AMD than patients with the more common protective TT genotype (encoding Y402), while

heterozygotes for the risk allele have a 2.5-4 fold increased risk. The risk (C) allele is very common, with an allele frequency of 35% and may contribute over half of all AMD cases<sup>95</sup>,<sup>96</sup>. However, direct evidence for functional consequences of this polymorphism remains elusive. I here show that the purified CFH H402 variant exhibits severely impaired binding to MDA, irrespective of the presence of an intact MDA binding site in SCR20 of the full-length protein. Remarkably, I could demonstrate gene-dosage dependent binding to MDA using whole plasma as a source of CFH. This correlates very well with the risk for developing AMD, which is already increased in patients heterozygous for the H402 variant albeit increased to a proportionately greater degree in homozygous patients. The 402H variant has also been reported to exhibit reduced binding to glycosaminoglycans and it has been suggested that merely the decreased presence of CFH at these sites favors increased complement activation<sup>97</sup>. In contrast to glycosaminoglycans, MDA is enriched in the membranes of dying cells, which are continuously generated in the retina and need to be efficiently removed<sup>98</sup>. I now demonstrate that the decreased MDA-binding capacity of the purified H402 variant leads to dramatically reduced generation of anti-inflammatory iC3b fragments on MDA-bearing surfaces. This provides a functional explanation for the strong disease association of the H402 variant, because reduced C3b inactivation on the surface of dying cells expressing MDA epitopes would result in complement propagation and excessive inflammation. Further support for a link between complement regulation and oxidative stress comes from the observation that the genetic risk conferred by the H402 variant is significantly reduced by the dietary intake of antioxidants<sup>99</sup>.

Consistent with an earlier report, I observed the presence of MDA epitopes throughout the choroid and Bruch's membrane including drusen of patients with AMD<sup>30</sup>. However, even under physiological conditions, oxidized phospholipids are formed as a result of photic stimulation of retinal photoreceptors and subsequently scavenged by a variety of processes including clearance via CD36<sup>100</sup>. As one of the major degradation products of peroxidized phospholipids, MDA is continuously generated. Therefore, physiological housekeeping mechanisms are critically needed to prevent accumulation of products of lipid peroxidation and adverse reactions mediated by them. My immunohistochemical results support a role for CFH, because I identified CFH in the same locations as MDA in patients with and without AMD. Although the same products are generated in other diseases, such as atherosclerosis, these homeostatic mechanisms may be particularly limiting factors in the eye.

Intriguingly, several lipid peroxidation products, including MDA, can cause retinal pigment epithelium damage accompanied by chronic inflammation<sup>101</sup>. I show here that MDA adducts have the capacity to induce IL-8 secretion in THP-1 cells. In retinal pigment epithelium cells, the central cell type involved in AMD, MDA-adducts induced IL-8 in a similar fashion, while at the same time mounting an antioxidant response. Consistent with this, IL-8 has been shown to be released by retinal pigment epithelial cells after ingestion of oxidized photoreceptors<sup>83</sup>. Increased IL-8 expression correlates with higher incidence of AMD, underlining its important pathogenic role<sup>102</sup>. Therefore, neutralization of MDA-adducts by CFH has the potential to limit several pathogenic events in AMD (Fig. 17). Indeed, I demonstrate that MDA-adducts also induce KC-expression in the RPE/choroid of mice *in vivo*, and this effect is blocked by co-administration of CFH.

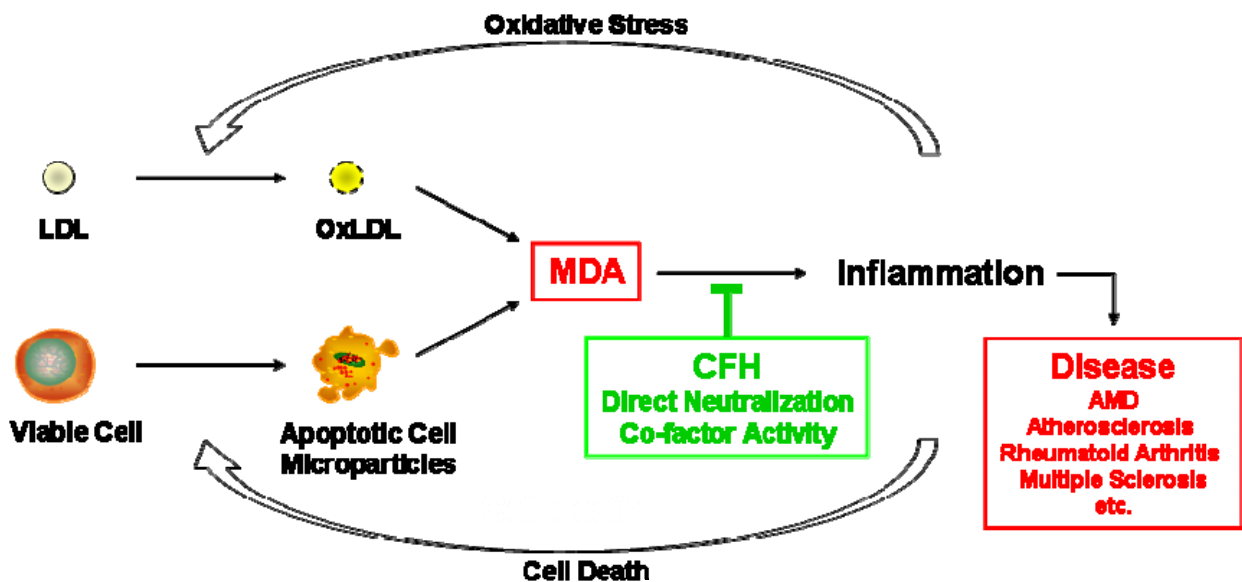


**Fig. 17: CFH - a novel innate defense mechanism against the consequences of oxidative stress**

CFH inhibits MDA-induced inflammation and thereby has the potential to break the vicious cycle of oxidative stress, inflammation and disease.

In summary: MDA is a common decomposition product of lipid peroxidation and is ubiquitously formed in a variety of both physiological and pathophysiological processes. I now identify CFH as a major MDA binding protein that can block the binding of MDA-LDL to macrophages and neutralizes MDA-induced proinflammatory effects *in vitro* and *in vivo*. I also show that a common polymorphism in CFH that is carried by 35% of the population, and is strongly associated with AMD, dramatically inhibits the ability of CFH to bind MDA.

Moreover, I demonstrate that CFH leads to complement inactivation on MDA-decorated surfaces and that this protective activity is severely reduced with the AMD-associated risk variant. This provides evidence that the inability of the risk variant of CFH to bind MDA is causally linked to the etiology of AMD, in particular because enhanced lipid peroxidation has been demonstrated to be involved in the pathogenesis of AMD <sup>28</sup>. Furthermore, because MDA is ubiquitously generated in inflammatory settings, including atherosclerosis, my data suggest the binding of CFH to MDA as an important innate mechanism to limit consequences of lipid peroxidation in a wide variety of diseases. Although the association of rs1061170 with atherosclerosis is far less clear, at present I cannot exclude that other genetic variations of CFH or CFHR-proteins affect MDA-binding and thereby contribute to its pathogenesis <sup>103</sup>. These insights may provide novel approaches to exploit endogenous host defense mechanisms for the prevention and therapy of chronic inflammatory diseases.

## 7. FUTURE DIRECTIONS

The results presented here, while fulfilling the aim of this thesis and confirming the initial hypothesis, raise at the same time a plethora of new questions, some of which I will briefly discuss in the following.

In the future, the effect of the 402H risk variant needs to be evaluated with respect to MDA *in vivo*. To address this, intraocular injections of MDA could be performed in a CFH deficient mouse strain that transgenically expresses the risk variant. This strain has been created, but unfortunately was not accessible during this study<sup>104</sup>. Besides rs1061170, a number of other non-synonymous polymorphisms residing in the MDA-binding SCRs 7 and 20 have been implicated in disease<sup>105</sup>. The binding assay established for this thesis (shown in Fig. 9B) will also allow to test whether other known polymorphisms influence the MDA-binding properties of CFH. This may contribute to our understanding of the pathogenic events caused by variations in the CFH gene.

However, variations of the CFH gene do not affect other members of the CFH family that may bind to MDA equally. Indeed, I demonstrated MDA-binding for one example, namely CFHR1. Impaired MDA-binding of CFH may shift the balance towards CFHRs on MDA-decorated surfaces, an intriguing hypothesis which is supported by the results presented in Fig. 12F. Therefore, all CFHRs will be tested for their ability to bind MDA, as this may have profound consequences in local complement regulation and microbial infection<sup>106</sup>.

In addition, the data included in this manuscript show that MDA-adducts act as a proinflammatory stimulus in macrophages as well as in epithelial cells. How these cells sense the presence of MDA-epitopes and respond to them, is an issue that remains to be addressed. SR-A is important for the uptake of MDA-LDL by macrophages and contributes to atherogenesis<sup>86, 107, 108</sup>. Other scavenger receptors have been shown to promote sterile inflammation through interaction with toll-like receptors<sup>109</sup>. It remains to be seen if binding of MDA by SR-A contributes to the inflammatory response and whether the latter involves other PRRs. The systemic approach used for the identification of CFH as an MDA-binding plasma protein may be equally helpful for finding MDA-receptors in cell lysate. Furthermore, comprehensive analysis of transcriptional targets of MDA would help to identify signaling

pathways involved in the MDA-response. This could be achieved by performing a gene-expression microarray with MDA-treated macrophages.

Many infectious agents protect themselves from complement attack by recruiting CFH to their surface <sup>110</sup>. CFH binding to microbes may be mediated by epitopes that are structurally similar to MDA. This intriguing hypothesis of molecular mimicry between oxidation specific epitopes and microbial antigens is supported by the fact that PC is present on OxLDL as well as on the surface of certain bacteria and other microbes <sup>70</sup>. The presence of MDA-related epitopes on the surface of certain microbes could be verified using a set of MDA-specific antibodies. Competition assays will answer the question whether the same epitopes are also involved in CFH binding. If this holds true, it would allow the translation of my findings to several infectious diseases where CFH-binding is detrimental. One would then assume that individuals carrying the H402 risk allele may be protected from infection with pathogens whose propagation depends on CFH. On the other hand, MDA-specific antibodies or peptides blocking the binding of CFH to microbial surfaces would be predicted to have a beneficial effect.

By these means, we aim at further exploring the newly found connection between oxidative stress and the innate immune system, taking into account its dual role in host defense and homeostasis.

## 8. REFERENCES

1. Chou, M. Y. et al. Oxidation-specific epitopes are important targets of innate immunity. *J Intern Med* 263, 479-88 (2008).
2. Weiner, H. L. & Frenkel, D. Immunology and immunotherapy of Alzheimer's disease. *Nat Rev Immunol* 6, 404-16 (2006).
3. Cotran, R. S., Kumar, V. & Robbins, S. Robbins Pathologic Basis of Disease. W. B. Saunders Company, Philadelphia (1994).
4. Ross, R. Atherosclerosis--an inflammatory disease. *N Engl J Med* 340, 115-26 (1999).
5. Coussens, L. M. & Werb, Z. Inflammation and cancer. *Nature* 420, 860-7 (2002).
6. Chen, G. Y. & Nunez, G. Sterile inflammation: sensing and reacting to damage. *Nat Rev Immunol* 10, 826-37 (2010).
7. Esterbauer, H., Schaur, R. J. & Zollner, H. Chemistry and biochemistry of 4-hydroxynonenal, malonaldehyde and related aldehydes. *Free Radic Biol Med* 11, 81-128 (1991).
8. Chang, M. K. et al. Monoclonal antibodies against oxidized low-density lipoprotein bind to apoptotic cells and inhibit their phagocytosis by elicited macrophages: evidence that oxidation-specific epitopes mediate macrophage recognition. *Proc Natl Acad Sci U S A* 96, 6353-8 (1999).
9. Berliner, J. A., Subbanagounder, G., Leitinger, N., Watson, A. D. & Vora, D. Evidence for a role of phospholipid oxidation products in atherogenesis. *Trends Cardiovasc Med* 11, 142-7 (2001).
10. Miller, Y. I. et al. Oxidation-specific epitopes are danger-associated molecular patterns recognized by pattern recognition receptors of innate immunity. *Circ Res* 108, 235-48.
11. Boullier, A. et al. Phosphocholine as a pattern recognition ligand for CD36. *J Lipid Res* 46, 969-76 (2005).
12. Boullier, A. et al. The binding of oxidized low density lipoprotein to mouse CD36 is mediated in part by oxidized phospholipids that are associated with both the lipid and protein moieties of the lipoprotein. *J Biol Chem* 275, 9163-9 (2000).
13. Binder, C. J. et al. Innate and acquired immunity in atherogenesis. *Nat Med* 8, 1218-26 (2002).
14. Chang, M. K., Binder, C. J., Torzewski, M. & Witztum, J. L. C-reactive protein binds to both oxidized LDL and apoptotic cells through recognition of a common ligand: Phosphorylcholine of oxidized phospholipids. *Proc Natl Acad Sci U S A* 99, 13043-8 (2002).
15. Shaw, P. X. et al. Natural antibodies with the T15 idiotype may act in atherosclerosis, apoptotic clearance, and protective immunity. *J Clin Invest* 105, 1731-40 (2000).
16. Palinski, W. et al. Cloning of monoclonal autoantibodies to epitopes of oxidized lipoproteins from apolipoprotein E-deficient mice. Demonstration of epitopes of oxidized low density lipoprotein in human plasma. *J Clin Invest* 98, 800-14 (1996).
17. Chou, M. Y. et al. Oxidation-specific epitopes are dominant targets of innate natural antibodies in mice and humans. *J Clin Invest* 119, 1335-49 (2009).
18. Horie, K. et al. Immunohistochemical colocalization of glycoxidation products and lipid peroxidation products in diabetic renal glomerular lesions. Implication for glycoxidative stress in the pathogenesis of diabetic nephropathy. *J Clin Invest* 100, 2995-3004 (1997).
19. Dei, R. et al. Lipid peroxidation and advanced glycation end products in the brain in normal aging and in Alzheimer's disease. *Acta Neuropathol* 104, 113-22 (2002).
20. Sanchez Perez, M. J. et al. Lipid peroxidation and serum cytokines in acute alcoholic hepatitis. *Alcohol Alcohol* 41, 593-7 (2006).
21. Imai, Y. et al. Identification of oxidative stress and Toll-like receptor 4 signaling as a key pathway of acute lung injury. *Cell* 133, 235-49 (2008).
22. Haider, L. et al. Oxidative damage in multiple sclerosis lesions. *Brain*.

23. Shanmugam, N. et al. Proinflammatory effects of advanced lipoxidation end products in monocytes. *Diabetes* 57, 879-88 (2008).
24. Hecker, M. & Ullrich, V. On the mechanism of prostacyclin and thromboxane A2 biosynthesis. *J Biol Chem* 264, 141-50 (1989).
25. Ohya, T. Formation of a new 1,1,1 adduct in the reaction of malondialdehyde, n-hexylamine and alkanal under neutral conditions. *Biol Pharm Bull* 16, 137-41 (1993).
26. Tuma, D. J., Thiele, G. M., Xu, D., Klassen, L. W. & Sorrell, M. F. Acetaldehyde and malondialdehyde react together to generate distinct protein adducts in the liver during long-term ethanol administration. *Hepatology* 23, 872-80 (1996).
27. Xu, D. et al. Epitope characterization of malondialdehyde-acetaldehyde adducts using an enzyme-linked immunosorbent assay. *Chem Res Toxicol* 10, 978-86 (1997).
28. Hollyfield, J. G. et al. Oxidative damage-induced inflammation initiates age-related macular degeneration. *Nat Med* 14, 194-8 (2008).
29. Suzuki, M. et al. Oxidized phospholipids in the macula increase with age and in eyes with age-related macular degeneration. *Mol Vis* 13, 772-8 (2007).
30. Schutt, F., Bergmann, M., Holz, F. G. & Kopitz, J. Proteins modified by malondialdehyde, 4-hydroxynonenal, or advanced glycation end products in lipofuscin of human retinal pigment epithelium. *Invest Ophthalmol Vis Sci* 44, 3663-8 (2003).
31. Pascolini, D. et al. 2002 global update of available data on visual impairment: a compilation of population-based prevalence studies. *Ophthalmic Epidemiol* 11, 67-115 (2004).
32. Congdon, N. et al. Causes and prevalence of visual impairment among adults in the United States. *Arch Ophthalmol* 122, 477-85 (2004).
33. Friedman, D. S. et al. Prevalence of age-related macular degeneration in the United States. *Arch Ophthalmol* 122, 564-72 (2004).
34. Alfaro, D. V. et al. (eds.) Age-related macular degeneration: a comprehensive textbook. (2006).
35. de Jong, P. T. Age-related macular degeneration. *N Engl J Med* 355, 1474-85 (2006).
36. Risk factors associated with age-related macular degeneration. A case-control study in the age-related eye disease study: Age-Related Eye Disease Study Report Number 3. *Ophthalmology* 107, 2224-32 (2000).
37. Klein, R. J. et al. Complement factor H polymorphism in age-related macular degeneration. *Science* 308, 385-9 (2005).
38. Haines, J. L. et al. Complement factor H variant increases the risk of age-related macular degeneration. *Science* 308, 419-21 (2005).
39. Hageman, G. S. et al. A common haplotype in the complement regulatory gene factor H (HF1/CFH) predisposes individuals to age-related macular degeneration. *Proc Natl Acad Sci U S A* 102, 7227-32 (2005).
40. Edwards, A. O. et al. Complement factor H polymorphism and age-related macular degeneration. *Science* 308, 421-4 (2005).
41. Gold, B. et al. Variation in factor B (BF) and complement component 2 (C2) genes is associated with age-related macular degeneration. *Nat Genet* 38, 458-62 (2006).
42. Brooimans, R. A., van der Ark, A. A., Buurman, W. A., van Es, L. A. & Daha, M. R. Differential regulation of complement factor H and C3 production in human umbilical vein endothelial cells by IFN-gamma and IL-1. *J Immunol* 144, 3835-40 (1990).
43. Rivera, A. et al. Hypothetical LOC387715 is a second major susceptibility gene for age-related macular degeneration, contributing independently of complement factor H to disease risk. *Hum Mol Genet* 14, 3227-36 (2005).
44. Sakaue, T. et al. Factor H in porcine seminal plasma protects sperm against complement attack in genital tracts. *J Biol Chem* 285, 2184-92.
45. Tu, Z., Li, Q., Bu, H. & Lin, F. Mesenchymal stem cells inhibit complement activation by secreting factor H. *Stem Cells Dev* 19, 1803-9.
46. Esparza-Gordillo, J. et al. Genetic and environmental factors influencing the human factor H plasma levels. *Immunogenetics* 56, 77-82 (2004).

47. de Cordoba, S. R. & de Jorge, E. G. Translational mini-review series on complement factor H: genetics and disease associations of human complement factor H. *Clin Exp Immunol* 151, 1-13 (2008).
48. Harrison, R. A. & Lachmann, P. J. The physiological breakdown of the third component of human complement. *Mol Immunol* 17, 9-20 (1980).
49. Pangburn, M. K., Schreiber, R. D. & Muller-Eberhard, H. J. Human complement C3b inactivator: isolation, characterization, and demonstration of an absolute requirement for the serum protein beta1H for cleavage of C3b and C4b in solution. *J Exp Med* 146, 257-70 (1977).
50. Weiler, J. M., Daha, M. R., Austen, K. F. & Fearon, D. T. Control of the amplification convertase of complement by the plasma protein beta1H. *Proc Natl Acad Sci U S A* 73, 3268-72 (1976).
51. Whaley, K. & Ruddy, S. Modulation of the alternative complement pathways by beta 1 H globulin. *J Exp Med* 144, 1147-63 (1976).
52. Rodriguez de Cordoba, S., Esparza-Gordillo, J., Goicoechea de Jorge, E., Lopez-Trascasa, M. & Sanchez-Corral, P. The human complement factor H: functional roles, genetic variations and disease associations. *Mol Immunol* 41, 355-67 (2004).
53. Manuelian, T. et al. Mutations in factor H reduce binding affinity to C3b and heparin and surface attachment to endothelial cells in hemolytic uremic syndrome. *J Clin Invest* 111, 1181-90 (2003).
54. Oppermann, M. et al. The C-terminus of complement regulator Factor H mediates target recognition: evidence for a compact conformation of the native protein. *Clin Exp Immunol* 144, 342-52 (2006).
55. Meri, S. & Pangburn, M. K. Discrimination between activators and nonactivators of the alternative pathway of complement: regulation via a sialic acid/polyanion binding site on factor H. *Proc Natl Acad Sci U S A* 87, 3982-6 (1990).
56. Joiner, K. A. et al. Biochemical characterization of a factor produced by trypanosomes of *Trypanosoma cruzi* that accelerates the decay of complement C3 convertases. *J Biol Chem* 263, 11327-35 (1988).
57. Pangburn, M. K. & Muller-Eberhard, H. J. The alternative pathway of complement. *Springer Semin Immunopathol* 7, 163-92 (1984).
58. Pangburn, M. K., Ferreira, V. P. & Cortes, C. Discrimination between host and pathogens by the complement system. *Vaccine* 26 Suppl 8, I15-21 (2008).
59. Carreno, M. P., Labarre, D., Maillet, F., Jozefowicz, M. & Kazatchkine, M. D. Regulation of the human alternative complement pathway: formation of a ternary complex between factor H, surface-bound C3b and chemical groups on nonactivating surfaces. *Eur J Immunol* 19, 2145-50 (1989).
60. Kazatchkine, M. D., Fearon, D. T., Silbert, J. E. & Austen, K. F. Surface-associated heparin inhibits zymosan-induced activation of the human alternative complement pathway by augmenting the regulatory action of the control proteins on particle-bound C3b. *J Exp Med* 150, 1202-15 (1979).
61. Zipfel, P. F. & Skerka, C. FHL-1/reconectin: a human complement and immune regulator with cell-adhesive function. *Immunol Today* 20, 135-40 (1999).
62. Jozsi, M. & Zipfel, P. F. Factor H family proteins and human diseases. *Trends Immunol* 29, 380-7 (2008).
63. Hellwege, J. et al. Functional properties of complement factor H-related proteins FHR-3 and FHR-4: binding to the C3d region of C3b and differential regulation by heparin. *FEBS Lett* 462, 345-52 (1999).
64. Timmann, C., Leippe, M. & Horstmann, R. D. Two major serum components antigenically related to complement factor H are different glycosylation forms of a single protein with no factor H-like complement regulatory functions. *J Immunol* 146, 1265-70 (1991).
65. Scholl, H. P. et al. Systemic complement activation in age-related macular degeneration. *PLoS One* 3, e2593 (2008).

66. Bird, A. C. et al. An international classification and grading system for age-related maculopathy and age-related macular degeneration. The International ARM Epidemiological Study Group. *Surv Ophthalmol* 39, 367-74 (1995).
67. Oppermann, M. et al. Quantitation of components of the alternative pathway of complement (APC) by enzyme-linked immunosorbent assays. *J Immunol Methods* 133, 181-90 (1990).
68. Purcell, S. et al. PLINK: a tool set for whole-genome association and population-based linkage analyses. *Am J Hum Genet* 81, 559-75 (2007).
69. Skerka, C. et al. Defective complement control of factor H (Y402H) and FHL-1 in age-related macular degeneration. *Mol Immunol* 44, 3398-406 (2007).
70. Binder, C. J. et al. Pneumococcal vaccination decreases atherosclerotic lesion formation: molecular mimicry between *Streptococcus pneumoniae* and oxidized LDL. *Nat Med* 9, 736-43 (2003).
71. Habeeb, A. F. Determination of free amino groups in proteins by trinitrobenzenesulfonic acid. *Anal Biochem* 14, 328-36 (1966).
72. Palinski, W. et al. Antisera and monoclonal antibodies specific for epitopes generated during oxidative modification of low density lipoprotein. *Arteriosclerosis* 10, 325-35 (1990).
73. Lu, L. et al. Synthesis and structural characterization of carboxyethylpyrrole-modified proteins: mediators of age-related macular degeneration. *Bioorg Med Chem* 17, 7548-61 (2009).
74. Rosenfeld, M. E., Palinski, W., Yla-Herttuala, S., Butler, S. & Witztum, J. L. Distribution of oxidation specific lipid-protein adducts and apolipoprotein B in atherosclerotic lesions of varying severity from WHHL rabbits. *Arteriosclerosis* 10, 336-49 (1990).
75. Young, S. G., Witztum, J. L., Casal, D. C., Curtiss, L. K. & Bernstein, S. Conservation of the low density lipoprotein receptor-binding domain of apoprotein B. Demonstration by a new monoclonal antibody, MB47. *Arteriosclerosis* 6, 178-88 (1986).
76. Young, S. G., Smith, R. S., Hogle, D. M., Curtiss, L. K. & Witztum, J. L. Two new monoclonal antibody-based enzyme-linked assays of apolipoprotein B. *Clin Chem* 32, 1484-90 (1986).
77. Friguet, B., Chaffotte, A. F., Djavadi-Ohanian, L. & Goldberg, M. E. Measurements of the true affinity constant in solution of antigen-antibody complexes by enzyme-linked immunosorbent assay. *J Immunol Methods* 77, 305-19 (1985).
78. Li, H. et al. Inhibition of cytosolic phospholipase A(2) suppresses production of cholesteryl ester through the reesterification of free cholesterol but not formation of foam cells in oxidized LDL-stimulated macrophages. *Biol Pharm Bull* 31, 6-12 (2008).
79. Hughes, A. E. et al. A common CFH haplotype, with deletion of CFHR1 and CFHR3, is associated with lower risk of age-related macular degeneration. *Nat Genet* 38, 1173-7 (2006).
80. Jager, R. D., Mieler, W. F. & Miller, J. W. Age-related macular degeneration. *N Engl J Med* 358, 2606-17 (2008).
81. Takizawa, F., Tsuji, S. & Nagasawa, S. Enhancement of macrophage phagocytosis upon iC3b deposition on apoptotic cells. *FEBS Lett* 397, 269-72 (1996).
82. Amarilyo, G. et al. iC3b-opsonized apoptotic cells mediate a distinct anti-inflammatory response and transcriptional NF-kappaB-dependent blockade. *Eur J Immunol* 40, 699-709.
83. Higgins, G. T., Wang, J. H., Dockery, P., Cleary, P. E. & Redmond, H. P. Induction of angiogenic cytokine expression in cultured RPE by ingestion of oxidized photoreceptor outer segments. *Invest Ophthalmol Vis Sci* 44, 1775-82 (2003).
84. Thiele, G. M. et al. Malondialdehyde-acetaldehyde (MAA) modified proteins induce pro-inflammatory and pro-fibrotic responses by liver endothelial cells. *Comp Hepatol* 3 Suppl 1, S25 (2004).
85. Gillotte-Taylor, K., Boullier, A., Witztum, J. L., Steinberg, D. & Quehenberger, O. Scavenger receptor class B type I as a receptor for oxidized low density lipoprotein. *J Lipid Res* 42, 1474-82 (2001).
86. Shechter, I. et al. The metabolism of native and malondialdehyde-altered low density lipoproteins by human monocyte-macrophages. *J Lipid Res* 22, 63-71 (1981).
87. Zipfel, P. F. & Skerka, C. Complement regulators and inhibitory proteins. *Nat Rev Immunol* 9, 729-40 (2009).

88. Ollert, M. W., David, K., Bredehorst, R. & Vogel, C. W. Classical complement pathway activation on nucleated cells. Role of factor H in the control of deposited C3b. *J Immunol* 155, 4955-62 (1995).
89. Flierman, R. & Daha, M. R. The clearance of apoptotic cells by complement. *Immunobiology* 212, 363-70 (2007).
90. Trouw, L. A. et al. C4b-binding protein and factor H compensate for the loss of membrane-bound complement inhibitors to protect apoptotic cells against excessive complement attack. *J Biol Chem* 282, 28540-8 (2007).
91. Leffler, J. et al. Annexin-II, DNA, and histones serve as factor H ligands on the surface of apoptotic cells. *J Biol Chem* 285, 3766-76.
92. Mihlan, M., Stippa, S., Jozsi, M. & Zipfel, P. F. Monomeric CRP contributes to complement control in fluid phase and on cellular surfaces and increases phagocytosis by recruiting factor H. *Cell Death Differ* 16, 1630-40 (2009).
93. Savill, J., Dransfield, I., Gregory, C. & Haslett, C. A blast from the past: clearance of apoptotic cells regulates immune responses. *Nat Rev Immunol* 2, 965-75 (2002).
94. Chang, M. K. et al. Apoptotic cells with oxidation-specific epitopes are immunogenic and proinflammatory. *J Exp Med* 200, 1359-70 (2004).
95. Thakkestian, A. et al. Systematic review and meta-analysis of the association between complement factor H Y402H polymorphisms and age-related macular degeneration. *Hum Mol Genet* 15, 2784-90 (2006).
96. Donoso, L. A., Vrabcic, T. & Kuivaniemi, H. The role of complement Factor H in age-related macular degeneration: a review. *Surv Ophthalmol* 55, 227-46.
97. Clark, S. J. et al. His-384 allotypic variant of factor H associated with age-related macular degeneration has different heparin binding properties from the non-disease-associated form. *J Biol Chem* 281, 24713-20 (2006).
98. Green, W. R. & Enger, C. Age-related macular degeneration histopathologic studies. The 1992 Lorenz E. Zimmerman Lecture. *Ophthalmology* 100, 1519-35 (1993).
99. Ho, L. et al. Reducing the Genetic Risk of Age-Related Macular Degeneration With Dietary Antioxidants, Zinc, and  $\omega$ -3 Fatty Acids: The Rotterdam Study. *Arch Ophthalmol* 129, 758-66.
100. Sun, M. et al. Light-induced oxidation of photoreceptor outer segment phospholipids generates ligands for CD36-mediated phagocytosis by retinal pigment epithelium: a potential mechanism for modulating outer segment phagocytosis under oxidant stress conditions. *J Biol Chem* 281, 4222-30 (2006).
101. Kaemmerer, E., Schutt, F., Krohne, T. U., Holz, F. G. & Kopitz, J. Effects of lipid peroxidation-related protein modifications on RPE lysosomal functions and POS phagocytosis. *Invest Ophthalmol Vis Sci* 48, 1342-7 (2007).
102. Goverdhan, S. V. et al. Interleukin-8 promoter polymorphism -251A/T is a risk factor for age-related macular degeneration. *Br J Ophthalmol* 92, 537-40 (2008).
103. Sofat, R. et al. Genetic variation in complement factor H and risk of coronary heart disease: eight new studies and a meta-analysis of around 48,000 individuals. *Atherosclerosis* 213, 184-90.
104. Ufret-Vincenty, R. L. et al. Transgenic mice expressing variants of complement factor H develop AMD-like retinal findings. *Invest Ophthalmol Vis Sci* 51, 5878-87.
105. Boon, C. J. et al. The spectrum of phenotypes caused by variants in the CFH gene. *Mol Immunol* 46, 1573-94 (2009).
106. Skerka, C. & Zipfel, P. F. Complement factor H related proteins in immune diseases. *Vaccine* 26 Suppl 8, I9-14 (2008).
107. Suzuki, H. et al. A role for macrophage scavenger receptors in atherosclerosis and susceptibility to infection. *Nature* 386, 292-6 (1997).
108. Babaev, V. R. et al. Reduced atherosclerotic lesions in mice deficient for total or macrophage-specific expression of scavenger receptor-A. *Arterioscler Thromb Vasc Biol* 20, 2593-9 (2000).
109. Stewart, C. R. et al. CD36 ligands promote sterile inflammation through assembly of a Toll-like receptor 4 and 6 heterodimer. *Nat Immunol* 11, 155-61.

110. Zipfel, P. F. et al. Factor H family proteins: on complement, microbes and human diseases. *Biochem Soc Trans* 30, 971-8 (2002).

## 9. LIST OF ABBREVIATIONS

4-HNE	4-hydroxynonenal
AMD	age related macular degeneration
apoB	apolipoprotein B
BSA	bovine serum albumin
C#	complement component #
CEP	carboxyethylpyrrole
CFH	complement factor H
CFHR	complement factor H related protein
CNV	choroidal neovascularisation
CRP	c-reactive protein
CuOx	Copper sulfate–oxidized
ELISA	enzyme-linked immunosorbent assay
FAAB	2-formyl-3-(alkylamino)butanal
GA	geographic atrophy
GAG(s)	glycosaminoglycan(s)
IL-	interleukin-
KC	growth-regulated alpha protein
LDL	low-density lipoprotein
LDLR	low-density lipoprotein receptor
MAA	malondialdehyde-acetaldehyde
MAC	membrane attack complex
MBL	mannose-binding lectin
MDA	malondialdehyde
MDHDC	4-methyl-1,4-dihydropyridine-3,5-dicarbaldehyde
NAb(s)	Natural antibodies
NK-cells	natural killer cells
PBS	phosphate buffered saline
PMA	phorbol-myristate-acetate
PRR(s)	pattern recognition receptor(s)
PUFA(s)	polyunsaturated fatty acid(s)
RAG	recombination activating gene 1
RLU	relative light units
RPE	retinal pigment epithelium
SCR	short consensus repeat
SD	standard deviation
SEM	standard error of the mean
TBS	tris buffered saline
TNF	tumor necrosis factor

## **10. PUBLICATION BASED ON THE THESIS**

Weismann D, Hartvigsen K, Lauer N, Bennett KL, Scholl HPN, Charbel Issa P, Cano M, Brandstätter H, Tsimikas S, Skerka C, Superti-Furga G, Handa JT, Zipfel PF, Witztum JL, Binder CJ. **Complement Factor H binds malondialdehyde-epitopes and protects from oxidative stress.** Nature, in revision

## 11. ACKNOWLEDGEMENTS

First of all, I want to thank my wife Lara for her numerous scientific contributions to this project as well as for her personal support. My God of Small Things, thank you for always opening my eyes when I cannot see.

I want to express my gratitude to my supervisor Christoph J. Binder who has given me this exciting project and, importantly, allowed me to complete what was going beyond the initial scope. I appreciate that I was granted independence while receiving continuous feedback.

I thank all the colleagues in the lab that gave me support over the years. Again, I owe a great deal of gratitude to Larissa Reis-Weismann for being a marvellous bench neighbour. I benefited a lot from our discussions. However, I cannot help being glad now that they did not stay merely scientific. I am grateful to Karsten Hartvigsen, our colleague for too short a time. This project would not be without you and your knowledge about MDA. To Sandrine J. Tonon, thank you for your contributions during the early stages of our lab. Furthermore, I deeply thank Maria Ozsvar-Kozma for persistently maintaining optimal working conditions against all odds.

I give thanks to the members of my thesis-committee, Dentscho Kerjaschki and Giulio Superti-Furga for their time to guide me through my PhD.

I want to acknowledge all my external collaborators, in particular Joseph L. Witztum for his constant support as well as Peter F. Zipfel for bravely getting on board when the sails were not yet set. I am also thankful to James T. Handa, above all for unhesitatingly stepping into an unexpected breach.

I thank all CeMMies for their helpfulness and the good spirits.

Last but not least, I would like to acknowledge my parents, my sisters and my brother for having constantly supported me.

## **12. FUNDING**

This work was supported by the Austrian Academy of Sciences, a BRIDGE grant from the Austrian Research Promotion Agency, and the Fondation Leducq.

## 13. AUTHORS CURRICULUM VITAE

### Personal Information

---

<b>Name</b>	David Weismann, Mag. rer. nat.
<b>Date of Birth</b>	February 22 <sup>nd</sup> , 1982
<b>Nationality</b>	Austrian
<b>Address</b>	Ce-M-M- Center for Molecular Medicine of the Austrian Academy of Sciences c/o KILM Department of Laboratory Medicine Medical University of Vienna Lazarettgasse 14 1090 Vienna Austria
<b>E-mail</b>	david.weismann@meduniwien.ac.at

### Education

---

<b>2006-present</b>	Student in the self contained, international Ce-M-M- PhD program
<b>2000-2006</b>	Human biology at University of Vienna, Austria (2000- 2003, 2005-2006), and University of Rome TOR VERGATA, Italy (2004). Graduation to Mag. rer. nat. with distinction.
<b>2004</b>	European studies at the International Summer School of the University of Vienna, Strobl, Austria. Graduation with distinction.
<b>1992-2000</b>	Bundesgymnasium Vöcklabruck, Austria. Matura with distinction.

## Research Experience

---

<b>Oct 2006-present</b>	PhD student: "Identification of plasma proteins binding to malondialdehyde-adducts" Supervisor: Prof. Christoph J. Binder Ce-M-M- & Medical University of Vienna, Austria
<b>Nov 2010</b>	Research visit at Friedrich Schiller Universität, Jena, Germany. Laboratory of Prof. Peter F. Zipfel
<b>Jun 2009</b>	Research visit at University of California, San Diego, USA. Laboratory of Prof. Joseph L. Witztum
<b>Mar 2005 – Mar 2006</b>	Diploma student: "Analysis of protein phosphatase 2A (PP2A) biogenesis in yeast" Supervisor: Prof. Egon Ogris Inst. of Medical Biochemistry, Medical University of Vienna, Austria
<b>Jul 2004 – Aug 2004</b>	Practical training: Monitoring of industrial effluents. Environmental laboratory Employer: Lenzing AG, Austria
<b>Mar 2004 – Jun 2004</b>	Practical training: "The molecular mechanism of apoptosis induced by Vesicular Stomatitis Virus infection in human carcinoma cells" Supervisor: Prof. Gabriella Santoro Department of Biology, University of Rome Tor Vergata, Italy
<b>Oct 2003 – Feb 2004</b>	Practical training: "The molecular mechanism of apoptosis induced by endoplasmatic reticulum stress" Supervisor: Prof. Mauro Piacentini Department of Biology, University of Rome Tor Vergata, Italy

## Experimental Skills

---

**Mouse handling:** intraperitoneal, intranasal and intratracheal injection, peritoneal and bronchoalveolar lavage, organ preparation, cell isolation from various tissues.

**Tissue culture:** plasmid transfection, reporter assay, monoclonal antibody generation (fusion of lymphocytes and myeloma cells, establishment of antibody-producing, monoclonal hybridoma cell line), foam cell assay, cell adhesion assay, phagocytosis assay.

**Other:** ELISA, cell-based ELISA, western blot, flow cytometry, immunohistochemistry, RT-qPCR, oxidative protein modifications (MDA, 4-HNE, copper-sulfate oxidation), bead coupling, pulldown and immunoprecipitation, CFH cofactor assay, decay accelerating assay.

## Languages

---

<b>German</b>	mother tongue
<b>English</b>	fluent
<b>Italian</b>	fluent
<b>French</b>	advanced
<b>Spanish</b>	advanced

## Teaching

---

**Co-supervision:** Gerald Haas, MSc, B.Tech. (Master project: “Delineation of the cellular responses to MDA-modified proteins in macrophages”)

## Peer Review Publications

---

Weismann D, Hartvigsen K, Lauer N, Bennett KL, Scholl HPN, Charbel Issa P, Cano M, Brandstätter H, Tsimikas S, Skerka C, Superti-Furga G, Handa JT, Zipfel PF, Witztum JL, Binder CJ. **Complement Factor H binds malondialdehyde-epitopes and protects from oxidative stress.** *In revision.*

Hombauer H, Weismann D, Mudrak I, Stanzel C, Fellner T, Lackner DH, Ogris E. **Generation of active protein phosphatase 2A is coupled to holoenzyme assembly.** *PLoS Biol.* 2007 Jun;5(6):e155.

## Competitive Scholarships

---

<b>2010</b>	Scholarship for the Keystone Symposium “Advances in Molecular Mechanisms of Atherosclerosis (J7)”
<b>2003</b>	ERASMUS scholarship Università degli studi di Roma TOR VERGATA
<b>2002</b>	Scholarship for European Studies at the Internationale Sommerhochschule der Universität Wien

## Conferences

---

<b>2010</b>	Keystone Symposium “Advances in Molecular Mechanisms of Atherosclerosis (J7)”, Banff, Canada. <i>Poster and oral presentation.</i>
<b>2008</b>	European Vascular Genomics Network Summer School, Cracow, Poland. <i>Poster presentation.</i>
<b>2008</b>	Young Scientist Association Conference, Medical University of Vienna, Austria. <i>Poster presentation.</i>
<b>2007</b>	Federation of the Societies of Biochemistry and Molecular Biology (FEBS) Meeting, Vienna, Austria.